



國立臺灣大學生命科學院生化科學研究所

碩士論文

Graduate Institute of Biochemical Science

College of Life Science

National Taiwan University

Master Thesis

細菌的十一異戊基二烯焦磷酸合成酶之抑制劑的合成
與評測

Synthesis and Evaluation of Bacterial Undecaprenyl
Diphosphate Synthase Inhibitors

陳曉萱

Hsiao-Hsuan Chen

指導教授：梁博煌 博士

Advisor: Po-Huang Liang, Ph.D.

中華民國 108 年 6 月

June, 2019



國立臺灣大學 (碩) 博士學位論文
口試委員會審定書

細菌的十一異戊基二烯焦磷酸合成酶之抑制劑的合成與
評測

Synthesis and Evaluation of Bacterial Undecaprenyl
Diphosphate Synthase Inhibitors

本論文係陳曉萱君(R06B46007)在國立臺灣大學生化科學研究所
完成之碩士學位論文，於民國 108 年 06 月 18 日承下列考試委員審查
通過及口試及格，特此證明。

口試委員：

Handwritten signature in blue ink, likely belonging to the convener of the oral exam committee.

(簽名)

(召集人)

Handwritten signature in blue ink, likely belonging to a member of the oral exam committee.

Handwritten signature in blue ink, likely belonging to the supervisor of the thesis.

(指導教授)

誌謝


光陰似箭，一晃眼兩年的時間就這麼匆匆的溜走，但也留下許多深遠的回憶。

一路上因為眾人的協助，我才能完成碩士學位。首先最該感謝的人莫過於我的父母，給予我極大的包容與支持，讓我可以勇敢地闖蕩我的夢想，累了還可以躲回他們築起的避風港休息。謝謝梁博煌老師，願意給予我機會進入實驗室學習，在每周會議時適時提出建議及修正方向。謝謝實驗室的眾多夥伴們，豐富了我的研究生生活；謝謝彥瑾學姊除了給予實驗上的建議外也指引我一些人生的方向，滿足生理及心理上的溫飽；Vathan, thank you for teaching me organic chemistry synthesized experiment and NMR. 謝謝俊宇學長在蛋白質純化、酵素動力學實驗上給予很多建議，以及期中期末考前的大惡補；謝謝玉如、瑾融兩個買午餐及玩耍的好夥伴，因為你們枯燥的實驗生活不再乏味；謝謝雍曄常聽我碎碎念，無論在課業或實驗上都是學習的好夥伴；謝謝明憲每周會議時提供的精闢見解及實驗上的小秘笈；謝謝有緯在學術論文寫作課程上的合作學習。謝謝聖偉學長協助貴重儀器的使用也在蛋白質實驗方面提供許多有用的見解；謝謝鄧怡君小姐提供測量Mass上的協助；謝謝所上的同學們這兩年來的協助與鼓勵。最後我要謝謝我的男友，包容我陪我談心紓解實驗上的不如意；也謝謝子凡姊，大學畢業後還繼續陪伴我，陪我聊很多心事，還提供我很多有機實驗方面的幫助。

其實有太多太多的感謝，真的無法以短短幾行字簡單帶過，只好將一切點滴記在心頭。


陳曉萱 謹誌於
國立台灣大學生化科學所
中華民國 一零八年六月

摘要



耐甲氧西林金黃色葡萄球菌 (methicillin-resistant *Staphylococcus aureus*) 等具多重抗藥性的金黃色葡萄球菌，是種致命且需要新的抗生素治療的醫院感染細菌。十一異戊基二烯焦磷酸合成酶 (undecaprenyl diphosphate synthase, UPPS) 將八當量的異戊烯基焦磷酸 (isopentenyl pyrophosphates, IPP) 與一當量的法尼基焦磷酸 (farnesyl pyrophosphate, FPP) 聚合，形成十一異戊基二烯焦磷酸 (undecaprenyl diphosphate, UPP)，是用於合成細菌細胞壁的肽聚糖的必要前驅物，因此十一異戊基二烯焦磷酸合成酶可作為新抗生素的標靶。基於十一異戊基二烯焦磷酸合成酶之結構和先前的研究，我們設計了一系列吡咯烷酮的衍生物，並使用法尼基焦磷酸的螢光衍生物 MANT-O-GPP 的活性測試法來測試它們對大腸桿菌及金黃色葡萄球菌之十一異戊基二烯焦磷酸合成酶的抑制作用，其中具有鹵素或苯基的化合物對抑制十一異戊基二烯焦磷酸合成酶更有效，而最小抑菌濃度的測試結果表明它們具有抑制枯草桿菌 (*Bacillus subtilis*) 的活性，根據酵素動力學和結構模擬，這些化合物對十一異戊基二烯焦磷酸合成酶而言是混合型的抑制劑。

ABSTRACT



The multiple antibiotic-resistant *Staphylococcus aureus*, such as methicillin-resistant *Staphylococcus aureus* (MRSA), is a fatal nosocomial infection that needs new antibiotics. Undecaprenyl diphosphate synthase (UPPS) condenses a farnesyl pyrophosphate (FPP) with eight isopentenyl pyrophosphates (IPP) to form undecaprenyl diphosphate (UPP) for the biosynthesis of peptidoglycan essential for bacterial cell wall, so it is a potential drug target for antibiotic. Based on UPPS structure and previous research, we designed a series of 4-carboxy-1-(4-styrylcarbonylphenyl)-2-pyrrolidinone derivatives and used a fluorescent analog of FPP, MANT-O-GPP, to test their inhibition on *E. coli* and MRSA UPPS. The compounds with halogen or benzene group were more potent to inhibit UPPS. Then, the EC₅₀ test showed that they have anti-bacterial activities to *Bacillus subtilis*. According to the enzyme kinetics and modeling, these compounds were mixed inhibitors of UPPS.



CONTENTS

摘要	I
ABSTRACT	II
CONTENTS	III
LIST OF SCHEME & TABLE	VI
LIST OF FIGURE	VII
ABBREVIATIONS	VIII
1 INTRODUCTION	1
1.1 Pathogens	1
1.2 Antibiotics and resistance	1
1.3 Undecaprenyl pyrophosphate synthase as a potential antibiotic target	3
1.4 Purpose of study	4
2 MATERIALS AND METHODS	5
2.1 Chemicals	5
2.2 Synthesize the inhibitor of UPPS	5
2.2.1 Synthesis of 1-(4-Acetylphenyl)-4-carboxy-2-pyrrolidinone (1)	5
2.2.2 General procedure of 4-Carboxy-1-(4-styrylcarbonylphenyl)-2-pyrrolidinones (2a-j)	6



2.3 <i>Sa</i> UPPS cloning.....	12
2.4 Purification of His-tagged <i>Ec</i> UPPS or <i>Sa</i> UPPS and removal of the tag.....	13
2.5 Kinetic measurements	14
2.5.1 General procedure.....	14
2.5.2 Extinction coefficient of MANT-O-GPP elongated product formation	15
2.5.3 Kinetic constant measurements	15
2.5.4 <i>Ec</i> UPPS and <i>Sa</i> UPPS inhibition assays	16
2.5.5 Measure the inhibited type of compounds.....	16
2.6 Antibacterial experiments	17
2.7 Docking compound in <i>Sa</i> UPPS.....	18
3 RESULT	19
3.1 Synthesis of pyrrolidinone derivatives	19
3.1.1 1-(4-Acetylphenyl)-4-carboxy-2-pyrrolidinone (1).....	19
3.1.2 4-Carboxy-1-(4-styrylcarbonylphenyl)-2-pyrrolidinones derivatives (2a-j)	19
3.2 Purification of UPPS	20
3.3 Kinetic constant of UPPS	21
3.4 Compound 2a-j inhibit UPPS activity	22
3.5 Antibacterial activity of compound 2d, i, j	23

3.6 Compound 2d was a mixed inhibitor.....	24
3.7 Compound 2d docked in the activity site of UPPS with FPP.....	24
4 DISCUSSION.....	26
TABLE.....	29
FIGURE.....	32
REFERENCE	45
SPECTURM.....	52



LIST OF SCHEME & TABLE



Scheme 1. Synthesize the derivatives of pyrrolidinone..... 20

Table 1. The kinetic constants of *Ec*UPPS and *Sa*UPPS..... 29

Table 2. The IC_{50} of compounds against *Ec*UPPS and *Sa*UPPS..... 30

Table 3. The EC_{50} values of compound 2d, i, and j..... 31



LIST OF FIGURE

Figure 1. The pathway of peptidoglycan synthesis.	3
Figure 2. SDS-PAGE analysis of the purified <i>Ec</i> UPPS and <i>Sa</i> UPPS.	33
Figure 3. The extinction coefficient of MANT-O-GPP convert to product.	33
Figure 4. The kinetic constant of <i>Ec</i> UPPS.	34
Figure 5. The kinetic constant of <i>Sa</i> UPPS.	35
Figure 6. The inhibition assay for <i>Ec</i> UPPS.	38
Figure 7. The inhibition assay for <i>Sa</i> UPPS.	41
Figure 8. The EC ₅₀ of compound 2d, I and j against <i>B. subtilis</i>	42
Figure 9. Compound 2d is a mixed inhibitor of <i>Sa</i> UPPS.	43
Figure 10. Docking of compound 2d in <i>Sa</i> UPPS with FPP.	44



ABBREVIATIONS

DMSO, dimethyl sulfoxide;

Da, Dalton;

EA, Ethyl acetate;

EC₅₀, Half maximal effective concentration

EcUPPS, *Escherichia coli* undecaprenyl pyrophosphate synthase;

EtBr, ethidium bromide;

FPP, farnesyl pyrophosphate;

IPP, isopentenyl pyrophosphate;

UPP, undecaprenyl pyrophosphate;

UPPS, undecaprenyl pyrophosphate synthase;

Hepes, 4-(2-hydroxyethyl)-1-piperazineethanesulfonic acid;

IC₅₀, half maximal inhibitory concentration;

IPTG, isopropyl-β-thiogalactopyranoside;

MANT-O-GPP,

(2E,6E)-8-O-(N-methyl-2-aminobenzoyl)-3,7-dimethyl-2,6-octandien-1-pyrophosphate;

mp, melting temperature;

MRSA, methicillin-resistant *Staphylococcus aureus*;

Ni-NTA, nickel nitrilo-tri-acetic acid;

NMR, nuclear magnetic resonance;

PCR, polymerase chain reaction;

*Sa*UPPS, *Staphylococcus aureus* undecaprenyl pyrophosphate synthase;

SDS-PAGE, sodium dodecyl sulfate-polyacrylamide gel electrophoresis;

TLC, thin-layer chromatography;

Tris, tris(hydroxymethyl)aminomethane





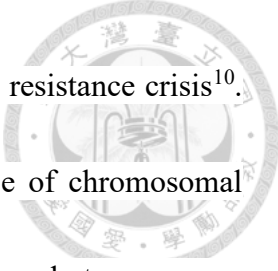
1 INTRODUCTION

1.1 Pathogens

Pathogens are microorganisms which can infect humans and cause diseases and death, such as bacteria, fungi, viruses¹. Among them, the most common are bacteria. Pathogenic bacteria often infect humans with compromised immunity. One of the most terrifying bacteria is *Mycobacterium tuberculosis* which caused tuberculosis and killed about 2 million people a year, mostly in sub-Saharan Africa². Other significant bacterias are Streptococcus and Pseudomonas which cause pneumonia, and Shigella, Campylobacter, and Salmonella which cause foodborne illnesses³⁻⁴. Pathogenic bacteria also cause diseases such as tetanus, typhoid fever, diphtheria, syphilis, and leprosy⁵.

1.2 Antibiotics and resistance

Bacteria can be killed by antibiotics. The first commercialized antibiotic, penicillin, was discovered by Alexander Fleming⁶ in 1928. It is a β -lactam interrupts the formation of peptidoglycan cross-linkages in the bacterial cell wall⁷. However, a few years later, a β -lactamase emerged in some bacteria to destroy and abolish the effect of penicillin. In 1960, scientists developed its derivatives, such as methicillin and carbapenem, which are less active toward β -lactamase⁸⁻⁹. Unfortunately, one year later, methicillin-resistant *Staphylococcus aureus* (MRSA) appeared and again brought a



deadly threat to humans⁸. In 1992, scientists have noticed antibiotics resistance crisis¹⁰. As reported, bacteria had resistance to antimicrobial agents because of chromosomal changes or the exchange of genetic materials via plasmids and transposons. *Streptococcus pneumoniae*, *Streptococcus pyogenes*, and *staphylococci* which cause respiratory and cutaneous infections, and members of the *Enterobacteriaceae* and *Pseudomonas* families, organisms which cause diarrhea, urinary infection, and sepsis, are resistant to all of the older antibiotics. The extensive use of antibiotics in the community and hospitals make this crisis even more serious. In 2008, Rice recommended “the ESKAPE bugs” referred to the six common antibiotic-resistant bacteria *Enterococcus faecium*, *Staphylococcus aureus*, *Klebsiella pneumoniae*, *Acinetobacter baumannii*, *Pseudomonas aeruginosa*, and *Enterobacter* species in hospitals¹¹. Then, scientists sought other targets to fight resistant bacteria. For example, linezolid approved for commercial use in 2000 is an antibiotic used to treat Gram-positive bacteria that are resistant to other antibiotics. It binds to the 50S subunit of the prokaryotic ribosome and prevents the initiated complex forming for protein synthesis forming¹². Other targets including the enzymes or elements participating cell wall biosynthetic pathways are being explored¹³⁻¹⁷.



1.3 Undecaprenyl pyrophosphate synthase as a potential antibiotic target

Undecaprenyl pyrophosphate synthase, UPPS, catalyzes consecutive condensation of eight molecules of isopentenyl diphosphate (IPP) with farnesyl diphosphate (FPP) to form UPP. It belongs to a prenyltransferase family which transfers prenyl groups to acceptors and participates in isoprenoid biosynthetic pathways¹⁸. UPP then acts as a lipid carrier for bacterial peptidoglycan biosynthesis¹⁹⁻²¹. This pathway of peptidoglycan synthesis is shown in Figure 1²². Due to its pivotal role in cell wall biosynthesis, UPPS has been suggested as a potential antibiotic target²³⁻³².

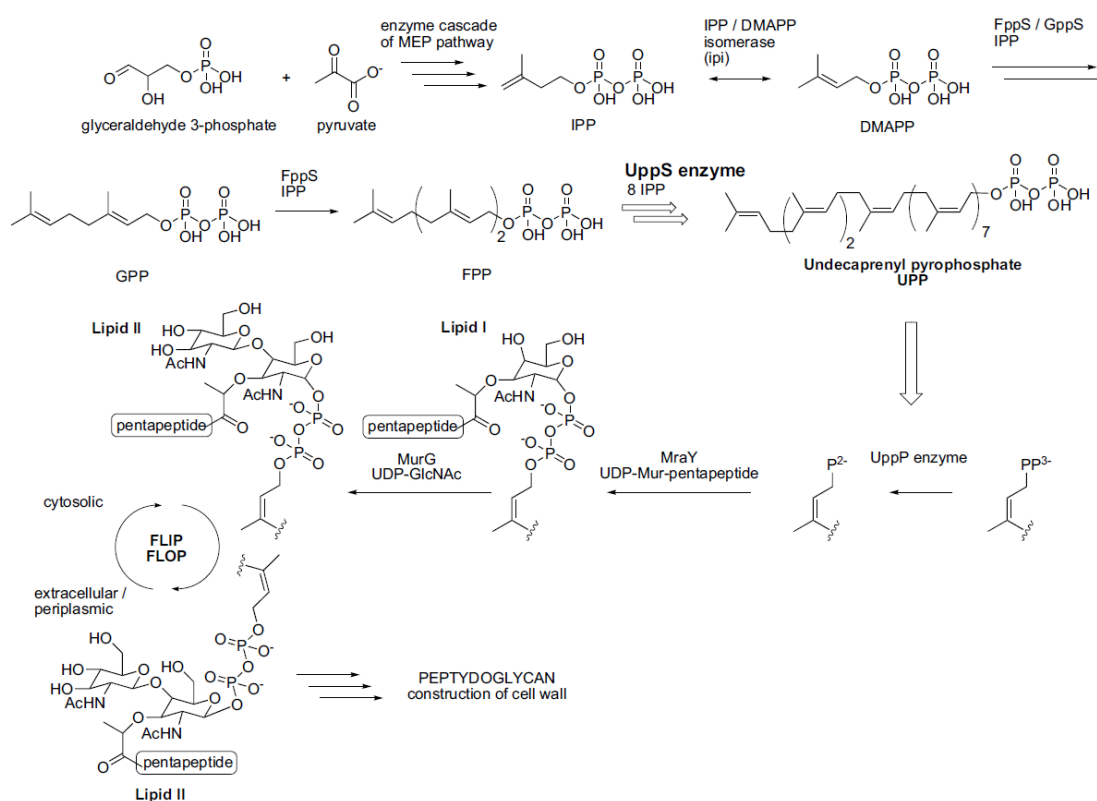



Figure 1. The pathway of peptidoglycan synthesis.

1.4 Purpose of study



Based on the rationale, we wanted to design inhibitors against UPPS and evaluated them. A previous postdoctor in our laboratory, Dr. Vathan Kumar, discovered a hit **VK-278** he synthesized to inhibit UPPS. Following his discovery, I synthesized its analogues and measured their inhibition on UPPS. We chose *E. coli* and *S. aureus* UPPS as working subjects because *S. aureus* is a Gram-positive resistant species and *E. coli* is a Gram-negative bacterium for comparison. We used a fluorescent analogue of FPP, MANT-O-GPP, to monitor the activity of UPPS because of its fluorescent increase at 420 nm during chain elongation³³⁻³⁴. We also investigated their types of inhibition with steady-state kinetic measurements at different substrate and inhibitor concentrations and docking by iGEMDOCK. Then, the compounds with better inhibition on UPPS enzymes were tested for inhibiting bacterial growth.



2 MATERIALS AND METHODS

2.1 Chemicals

4- aminoacetophenone, itaconic acid, 4-bromobenzaldehyde, 4-cyanobenzaldehyde, 3-cyanobenzaldehyde, 3-nitrobenzaldehyde, 4-biphenylcarboxaldehyde, and 3,4-dichlorobenzaldehyde were purchased from AK Scientific (Union City, USA). Benzaldehyde, 4-chlorobenzaldehyde, and 4-carboxybenzaldehyde were purchased from Acros Organics (New Jersey, USA). 4-fluorobenzaldehyde was purchased from Alfa Aesar (Ward Hill, USA). GenepHlow™ Gel/PCR kit was purchased from Geneaid (Taiwan). TLC, pET-32 Xa/LIC Vector Kit, and Ni-NTA were purchased from Merck (Darmstadt, Germany). Thrombin was purchased from GE Healthcare (Chicago, United States). MANT-O-GPP was synthesized previously in our laboratory. IPP was purchased from Echelon Biosciences (Salt Lake City, USA).

2.2 Synthesize the inhibitor of UPPS

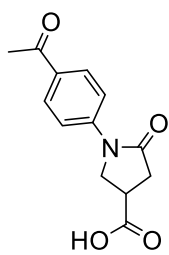
2.2.1 Synthesis of 1-(4-Acetylphenyl)-4-carboxy-2-pyrrolidinone (1)

A mixture of 1 g (7.40 mmol) 4-aminoacetophenone and 1.2 g (8.89 mmol) itaconic acid was stirred and heated (110-130 °C) under reflux for 18 hours. The progress of the reaction was monitored by TLC. After cooling to room temperature, 10 ml methanol was added to the reaction mixture. The reaction mixture was sonicated and

heated to dissolve in methanol, then cooled to room temperature to wait for recrystallization. Crystallization was filtered and washed with EA to yield the product.

The product was dissolved in the DMSO-d₆ to test NMR by Bruker AVIIIHD 400MHz FT-NMR in the department of chemistry, National Taiwan University (Taiwan) and was dissolved in the methanol for mass measurement by Bruker UPLC-MS in the College of Life Science (TechComm, National Taiwan University, Taiwan) to confirm the product. Then, the product was measured its melting temperature by Fargo MP-1D Melting Point Apparatus in our lab.

1-(4-Acetylphenyl)-4-carboxy-2-pyrrolidinone (1)



White solid, Yield : 49.8 %, mp 180-181 °C, ¹H NMR (400 MHz, DMSO-d₆) δ: 2.54 (s, 3H), 2.70-2.85 (m, 2H), 3.33-3.40 (m, 1H), 3.99-4.12 (m, 2H), 7.80, 7.96 (2d, J=8.9 Hz, 4H), ¹³C NMR (100 MHz,

DMSO-d₆) δ: 26.5, 35.0, 35.3, 49.8, 118.4, 129.2, 132.1, 143.1, 172.6, 174.0, 196.6,

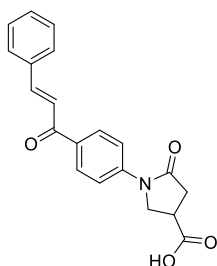
MS m/z : [M+H]⁺ = 248.09 (calcd. for C₁₃H₁₃NO₄ 248.09)

2.2.2 General procedure of 4-Carboxy-1-(4-styrylcarbonylphenyl)-2-pyrrolidinones (2a-j).

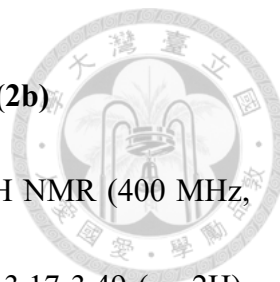
1-(4-Acetylphenyl)-4-carboxy-2-pyrrolidinone **1** 0.1g (0.40 mmol) in 5 ml ethanol treated with 500 μl of 50% NaOH under magnetically stirred condition at room temperature was reacted with benzaldehyde (0.5 mmol). The mixture was stirred

magnetically until complete consumption of the starting material **1**. The progress of the reaction was monitored by TLC. After the reaction was completed, ethanol was removed under reduced pressure. The residue was dissolved in 10 ml ddH₂O. The solution was transferred to a separatory funnel and extracted with EA. The aqueous layer was collected and added 100 ml ice, then acidified with aq HCl to pH 1-2. The yellow precipitate was filtered and then washed with water³⁵. The products were dissolved in the DMSO-d₆ for NMR measurement and in the methanol for mass measurement to confirm the product. Then, the products were measured their melting temperature.

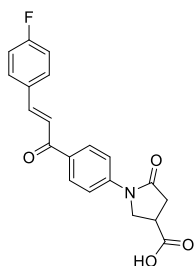
4-Carboxy-1-(4-styrylcarbonylphenyl)-2-pyrrolidinone (2a)



Light yellow solid, Yield : 70.0 %, mp 209-210 °C, ¹H NMR (400 MHz, DMSO-d₆) δ: 2.76-2.83 (m, 2H), 3.37-3.40 (m, 1H), 4.02-4.07 (m, 2H), 7.44-7.46 (m, 3H), 7.85-7.89 (m, 4H), 7.73, 7.75 (2d, J=15.6 Hz, 2H), 8.19 (d, J=9.0 Hz, 2H) 12.79 (s, 1H), ¹³C NMR (100 MHz, DMSO-d₆) δ: 35.0, 35.4, 49.8, 118.5, 121.9, 128.8, 128.9, 129.6, 130.5, 132.6921, 134.7, 143.2, 143.6, 172.6, 174.0, 187.7, MS m/z : [M+H]⁺ = 336.12 (calcd. for C₂₀H₁₇NO₄ 336.12)



1-[4-(4-fluorostyrylcarbonyl)phenyl]-4-carboxy-2-pyrrolidinone (2b)



Yellow solid, Yield : 42.4 %, mp 256-257 °C, ^1H NMR (400 MHz, DMSO- d_6) δ : 2.41-2.52 (m, 2H), 2.76 (m, 1H), 3.17-3.49 (m, 2H),

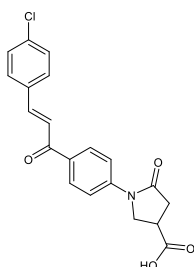
7.85 (d, $J=15.6$ Hz, 2H) 7.25-7.30 (m, 2H), 7.63 (d, $J=15.6$ Hz, 1H),

7.85 (d, $J=15.6$ Hz, 1H), 7.91-7.99 (m, 4H), ^{13}C NMR (100 MHz, d_6 -DMSO) δ : 36.1,

41.6, 44.4, 111.4, 116.1, 116.3, 122.7, 125.7, 131.1, 131.2, 131.4, 132.2, 140.5, 153.3,

174.2, 175.7, 186.2, MS m/z : $[\text{M}+\text{H}]^+ = 354.11$ (calcd. for $\text{C}_{20}\text{H}_{16}\text{FNO}_4$ 354.11)

1-[4-(4-chlorostyrylcarbonyl)phenyl]-4-carboxy-2-pyrrolidinone (2c)



Yellow solid, Yield : 20.5 %, mp 232-233 °C, ^1H NMR (400 MHz,

MeOD) δ : 2.58-2.78 (m, 2H), 3.13-3.16 (m, 1H), 3.42-3.62 (m, 2H),

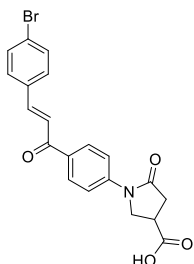
6.73 (m, $J=7.7$ Hz, 2H), 7.42 (d, $J=4$ Hz, 2H), 7.63-7.77 (m, 4H),

7.96 (d, $J=7.7$ Hz, 2H), ^{13}C NMR (100 MHz, MeOD) δ : 34.6, 42.5, 45.0, 112.6, 123.8,

127.3, 130.1, 130.8, 132.6, 135.4, 136.9, 142.4, 154.7, 175.4, 176.8, 189.6, MS m/z :

$[\text{M}+\text{H}]^+ = 370.08$ (calcd. for $\text{C}_{20}\text{H}_{16}\text{ClNO}_4$ 370.08)

1-[4-(4-Bromostyrylcarbonyl)phenyl]-4-carboxy-2-pyrrolidinone (2d)



Dark yellow solid, Yield : 75.0 %, mp 232-233 °C, ^1H NMR (400 MHz,

DMSO- d_6) δ : 2.72-2.87 (m, 2H), 3.34-3.41 (m, 1H), 4.02-4.15 (m, 2H),

7.64-7.71 (m, 3H), 7.83-7.86 (m, 4H), 7.99 (d, $J=15.6$ Hz, 1H), 8.19 (d,

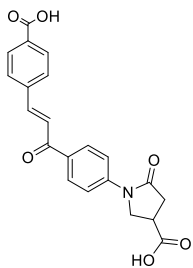
$J=8.9$ Hz, 2H) 12.76 (s, 1H), ^{13}C NMR (100 MHz, d_6 -DMSO) δ : 35.1, 35.4, 49.8, 118.5,



122.7, 123.9, 129.6, 130.8, 131.8, 132.6, 134.0, 142.2, 143.3, 172.7, 174.1, 187.5, MS

m/z : $[M+H]^+ = 413.03$ (calcd. for $C_{20}H_{16}BrNO_4$ 413.03)

1-[4-(4-carboxystyrylcarbonyl)phenyl]-4-carboxy-2-pyrrolidinone (2e)



Yellow solid, Yield : 38.0 %, mp 308-309 °C, 1H NMR (400 MHz,

MeOD) δ : 2.52-2.72 (m, 2H), 3.04-3.07 (m, 1H), 3.37-3.58 (m, 2H),

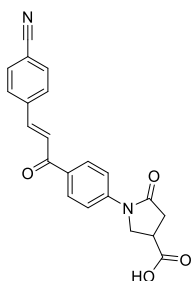
6.72 (d, $J=8.8$ Hz, 2H), 7.42 (d, $J=8.5$ Hz, 2H), 7.63-7.78 (m, 4H), 7.96

(d, $J=8.8$ Hz, 2H), ^{13}C NMR (100 MHz, MeOD) δ : 35.9, 43.4, 45.4, 112.6, 124.0, 127.2,

130.2, 130.9, 132.6, 135.5, 136.9, 142.4, 154.9, 176.8, 178.3, 189.6, MS m/z : $[M+H]^+ =$

380.11 (calcd. for $C_{21}H_{17}NO_6$ 380.11)

1-[4-(4-cyanostyrylcarbonyl)phenyl]-4-carboxy-2-pyrrolidinone (2f)



Yellow solid, Yield : 30.9 %, mp 250-251 °C, 1H NMR (400 MHz,

DMSO- d_6) δ : 2.67-2.79 (m, 2H), 3.03-3.12 (m, 1H), 4.01-4.05 (m, 2H),

7.73 (d, $J=15.6$ Hz, 1H), 7.86, 7.91 (2d, $J=8.3$ Hz, 4H), 8.08-8.10 (m,

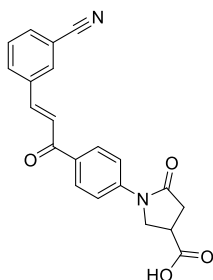
3H), 8.20 (d, $J=8.6$ Hz, 2H), ^{13}C NMR (100 MHz, DMSO- d_6) δ : 36.6,

51.2, 112.2, 118.3, 118.6, 125.3, 129.4, 129.8, 132.0, 132.7, 139.3, 141.2, 143.8, 174.0,

175.2, 187.5, MS m/z : $[M+H]^+ = 361.11$ (calcd. for $C_{21}H_{16}N_2O_4$ 361.11)



1-[4-(3-cyanostyrylcarbonyl)phenyl]-4-carboxy-2-pyrrolidinone (2g)

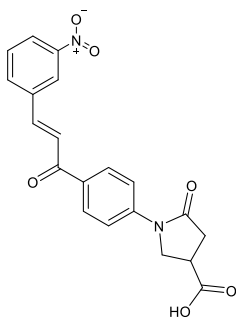


Light yellow solid, Yield : 34.6 %, mp 270-271 °C, ^1H NMR (400 MHz, DMSO- d_6) δ : 2.62-2.67 (m, 1H), 2.78-2.83 (m, 2H), 3.95-4.10 (m, 2H), 7.62-7.74 (m, 2H), 7.85-7.87 (m, 3H), 8.09-8.21 (m, 4H), 8.48 (s, 1H), ^{13}C NMR (100 MHz, DMSO- d_6) δ : 37.4, 37.6, 52.1,

112.1, 118.2, 118.5, 124.2, 129.7, 130.1, 131.9, 133.3, 133.6, 136.1, 140.9, 144.1, 174.8,

175.3, 187.4, MS m/z : $[\text{M}+\text{H}]^+ = 361.11$ (calcd. for $\text{C}_{21}\text{H}_{16}\text{N}_2\text{O}_4$ 361.11)

1-[4-(3-nitrostyrylcarbonyl)phenyl]-4-carboxy-2-pyrrolidinone (2h)

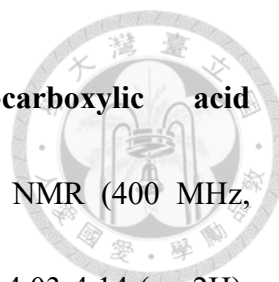


Light yellow solid, Yield : 30.2 %, mp 224-225 °C, ^1H NMR (400 MHz, DMSO- d_6) δ : 2.72-2.85 (m, 2H), 3.29-3.37 (m, 1H), 4.02-4.14 (m, 2H), 7.72-7.63 (m, 1H), 7.81-7.88 (m, 3H), 8.17 (d, $J=15.6$ Hz, 1H), 8.23-8.27 (m, 3H), 8.33 (d, $J=7.6$ Hz, 1H), 8.77 (s,

1H), ^{13}C NMR (100 MHz, DMSO- d_6) δ : 35.4, 35.6, 50.1, 118.5, 123.0, 124.6, 124.7,

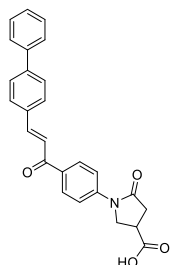
129.8, 130.3, 132.3, 135.0, 136.6, 141.0, 143.5, 148.4, 172.9, 174.2, 187.5, MS m/z :

$[\text{M}+\text{H}]^+ = 381.11$ (calcd. for $\text{C}_{20}\text{H}_{16}\text{N}_2\text{O}_6$ 381.11)



1-(4-(3-([1,1'-biphenyl]-4-yl)acryloyl)phenyl)-5-oxopyrrolidine-3-carboxylic acid

(2i) Yellow solid, Yield : 63.7 %, mp 280-281 °C, ¹H NMR (400 MHz,



DMSO-d₆) δ: 2.72-2.86 (m, 2H), 3.21-3.47 (m, 1H), 4.03-4.14 (m, 2H),

6.67-6.69 (d, J=8.60 Hz), 7.38-7.50 (m, 3H), 7.64-7.79 (m, 5H), 7.85-8.01

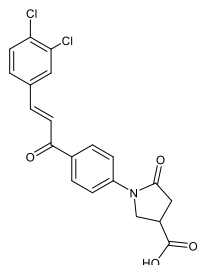
(m, 5H), 8.21 (d, J=8.7 Hz, 1H), ¹³C NMR (100 MHz, DMSO-d₆) δ:

35.3, 35.5, 50.02, 118.5, 121.8, 126.7, 127.0, 128.0, 129.0, 129.5, 129.6,

131.0, 132.7, 133.9, 139.2, 142.0, 143.1, 172.8, 174.2, 187.6, MS m/z : [M+H]⁺ =

412.15 (calcd. for C₂₆H₂₁NO₄ 412.15)

1-[4-(3,4-dichlorostyryl)carbonyl]phenyl]-4-carboxy-2-pyrrolidinone (2j)



Yellow solid, Yield : 20.7 %, mp 208-209 °C, ¹H NMR (400 MHz,

DMSO-d₆) δ: 2.44-2.58 (m, 2H), 2.82-2.88 (m, 1H), 3.26-3.47 (m, 2H),

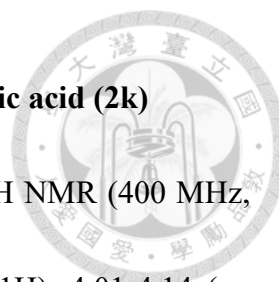
6.70 (d, J=8.8 Hz, 2H), 7.58 (d, J=15.5 Hz, 1H), 7.69-7.74 (m, 1H),

7.83-7.88 (m, 1H), 7.98-8.05 (m, 3H), 8.25 (d, J=1.8 Hz, 1H), ¹³C

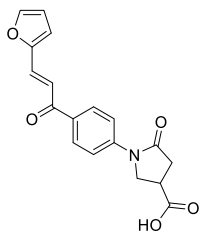
NMR (100 MHz, DMSO-d₆) δ: 34.8, 41.0, 43.8, 111.0, 124.6, 125.2, 128.8, 129.8,

130.8, 131.2, 131.7, 132.0, 136.1, 138.6, 153.0, 173.4, 174.9, 185.5, MS m/z : [M+H]⁺ =

404.05 (calcd. for C₂₀H₁₅Cl₂NO₄ 404.05)



1-(4-(3-(furan-2-yl)acryloyl)phenyl)-5-oxopyrrolidine-3-carboxylic acid (2k)



Brown solid, Yield : 52.5 %, mp 195-196 °C, ¹H NMR (400 MHz,

DMSO-d₆) δ: 2.72-2.87 (m, 2H), 3.34-3.40 (m, 1H), 4.01-4.14 (m,

2H), 6.68-6.69 (m, 1H), 7.09-7.10 (d, J=3.36 Hz, 1H), 7.55(s, 2H),

7.83-7.85 (d, J=8.88 Hz, 2H), 7.90 (d, J=1.16 Hz, 1H), 8.09-8.11 (d, J=8.8 Hz, 2H),

12.77 (s, 1H), ¹³C NMR (100 MHz, DMSO-d₆) δ: 35.0, 35.3, 49.8, 113.1, 116.9, 118.6,

129.3, 130.1, 132.6, 143.1, 146.1, 151.2, 172.6, 174.0, 187.1, MS m/z : [M+H]⁺ =

326.10 (calcd. for C₂₀H₁₅Cl₂NO₄ 326.10)

2.3 SaUPPS cloning

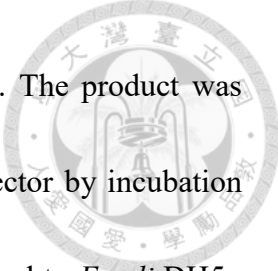
The gene of SaUPPS was synthesized by Bio Basic Inc. (Canada). The forward primer 5'-GGTATTGAGGGTCGCGAATTCGAGAACCTGTACTIONTCCAGGG-3'

(forward) and the backward primer

5'-AGAGGAGAGTTAGAGCCCTCGAGTTATTCCTCGCTCAGGCC-3' for PCR

reactions to amplify the gene were prepared by MISSION BIOTECH Inc. (Taiwan).

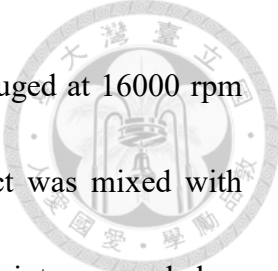
Thirty cycles of PCR reactions were performed using a thermocycler (Biometra) with the denaturing temperature at 94 °C for 30 s, melting temperature at 66 °C for 30 s, and the annealing temperature at 72 °C for 1 min. The PCR product was subjected to electrophoresis on 1% agarose gel with EtBr in TAE buffer. The correct band on the gel



was cut and the DNA was purified by GenepHlow™ Gel/PCR kit. The product was treated with T4 DNA Polymerase and annealed to pET32Xa/LIC vector by incubation at 22 °C for 5 min. The recombinant *SaUPPS* plasmid was transformed to *E.coli* DH5 α competent cells and spread on LB agar plate containing 100 μ g/mL ampicillin. An Ampicillin-resistant colony was selected and added to 5 mL fresh LB medium containing 100 μ g/mL ampicillin and incubated at 37 °C overnight. The sequence of *SaUPPS* in the plasmid was confirmed by MISSION BIOTECH Inc. (Taiwan)

2.4 Purification of His-tagged *EcUPPS* or *SaUPPS* and removal of the tag

The plasmid containing *EcUPPS* or *SaUPPS* gene and pET32Xa/LIC vector was transformed to *E.coli* BL21 (*DE3*) and spread on LB agar plate containing 100 μ g/mL ampicillin. A single colony was picked and added to 5 mL fresh LB medium containing 100 μ g/mL ampicillin and stirred at 37 °C overnight. The culture was transferred to 800 ml fresh LB medium containing 100 μ g/mL ampicillin and stirred at 37 °C. The cells were grown to OD₆₀₀ = 0.6 and the protein expression was induced with 1 mM IPTG. After 4 hours, the culture was centrifuged at 6000 rpm for 15 min. The supernatant was discarded and the cell paste was collected. The cell paste was suspended in 50 ml lysis buffer (pH7.5) containing 10 mM Tris-HCl, 500 mM NaCl, 10 mM imidazole, and 2 μ M 2-mercaptoethanol. The cells were disrupted with a French pressure cell press



(AIM-AMINCO spectronic Instruments). The cell lysate was centrifuged at 16000 rpm for 30 min at 4 °C to remove the cell debris. The cell-free extract was mixed with Ni-NTA resin which had been equilibrated with the lysis buffer. The mixture was shaken for 0.5-1 hour at 4 °C and then loaded into a column. After the Ni-NTA column was washed with the washing buffer (the lysis buffer plus 25 mM imidazole for 20-fold resin volume), the His-tagged *EcUPPS* or *SaUPPS* was eluted with 20 mL elution buffer (the lysis buffer plus 250 mM imidazole). The His-tagged protein-containing fractions were collected, concentrated and added with 10 µl thrombin to digest His-tag, then the mixture was put in a dialysis bag and dialyzed against the buffer containing 20 mM Tris-HCl, 150 mM NaCl, and 2 mM CaCl₂ overnight at 4 °C. The mixture in the bag was passed through a Ni-NTA column to collect the flow through as the purified tag-free *EcUPPS* or *SaUPPS*. SPS-PAGE was used to analyze the expression and purification effect of *EcUPPS* or *SaUPPS*.

2.5 Kinetic measurements

2.5.1 General procedure

All reactions were in 100 µL solutions with 100 mM Hepes-KOH buffer (pH 7.5), 50 mM KCl, 0.5mM MgCl₂, and 0.1% Triton X-100 with 0.1µM *EcUPPS* or 0.01 µM *SaUPPS* at 25 °C. The fluorescence change of MANT-O-GPP every 10 s in a total

period of 10 min was monitored by using a Hybrid Multi-Mode Reader (BioTeK Synergy™ H1) utilizing an excitation wavelength of 352 nm and an emission wavelength of 420 nm.

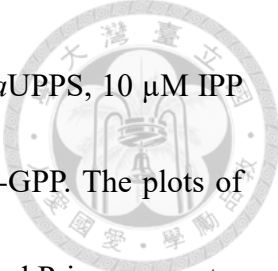


2.5.2 Extinction coefficient of MANT-O-GPP elongated product formation

The standard curve of the total fluorescence change versus the consumed MANT-O-GPP was used to calculate the extinction coefficient of MANT-O-GPP elongated product formation, which was used to calculate the initial rate of the UPPS reactions. To obtain this standard curve, 0.008, 0.016, 0.031, 0.063, 0.125, 0.25, 0.5 μM MANT-O-GPP were reacted with 30 μM IPP to yield difference levels of fluorescence increase. This plot was linear and the slope was used to give the extinction coefficient by excel.

2.5.3 Kinetic constant measurements

The kinetic constants were determined in 100 μL mixture with 0.1 μM *EcUPPS* or 0.01 μM *SaUPPS* and different substrate concentrations by monitoring their fluorescence changes. To measure the K_m and k_{cat} of IPP for *EcUPPS*, 2 μM MANT-O-GPP was used to saturate the enzyme and 1.88, 3.75, 7.5, 15, 30, 60, 120 μM IPP was used. To test K_m and k_{cat} of MANT-O-GPP for *EcUPPS*, 90 μM IPP was reacted with 0.03, 0.06, 0.125, 0.25, 0.5, 1, 1.5, 2 μM MANT-O-GPP. To test the K_m and k_{cat} of IPP for *SaUPPS*, 2 μM MAN-O-GPP reacted with 0.11, 0.23, 0.47, 0.94, 1.88,



3.75, 7.5, 15 μM IPP. To test the K_m and k_{cat} of MANT-O-GPP for *Sa*UPPS, 10 μM IPP reacted with 0.02, 0.03, 0.06, 0.125, 0.25, 0.5, 1, 1.5 μM MANT-O-GPP. The plots of initial rates versus substrate concentrations were analyzed by GraphPad Prism computer program. The data were fitted by non-linear regression of the Michaelis-Menten equation (eq.1) to obtain K_m and V_{max} values, then k_{cat} was calculated from $V_{\text{max}}/[E]$.

$$V_0 = V_{\text{max}} [S] / (K_m + [s]) \quad \text{eq.1}$$

2.5.4 *Ec*UPPS and *Sa*UPPS inhibition assays

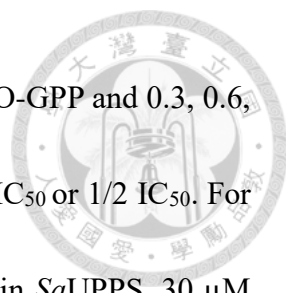
For measuring the IC_{50} values of compounds **2a-j** and **VK-278** on *Ec*UPPS or *Sa*UPPS, 0.1 μM *Ec*UPPS or 0.01 μM *Sa*UPPS was used in a reaction mixture containing MANT-O-GPP, IPP at the concentration of K_m , and various concentrations of the compound ranging from 0 to 100 μM . Stock solutions of compounds **2a-j** and **VK-278** were 10 mM in DMSO³⁴. IC_{50} values were obtained by fitting the plots of initial rates versus the concentrations of compounds **2a-j**, **VK-278** with Eq.2.

$$A(I) = A(0) \times [I] / ([I] + K_m) \quad \text{eq.2}$$

In this equation, $A(I)$ is the enzyme activity with an inhibitor concentration of I , $A(0)$ is the enzyme activity without inhibitor, and I is the concentration of inhibitor.

2.5.5 Measure the inhibited type of compounds

To test the inhibition type of compound **2d**, different concentrations of substrates and the compound were used to monitor the fluorescence changes. For the inhibition



type of compound **2d** with respect to IPP in *SaUPPS*, 2 μM MANT-O-GPP and 0.3, 0.6, 1.2, 2.4, 4.8 μM IPP were reacted without or with compound **2d** in IC_{50} or $1/2 \text{IC}_{50}$. For the inhibition type of compound **2d** with respect to MANT-O-GPP in *SaUPPS*, 30 μM IPP and 0.25, 0.5, 1, 1.5, 2 μM MANT-O-GPP were reacted without or with compound **2d** in $1/2 \text{IC}_{50}$ or IC_{50} . The initial rates of different substrate concentrations were calculated from the extinction coefficient by excel. Then, the plots of reciprocal of initial rates versus reciprocal of substrate concentrations were used to determine the inhibition patterns and the K_i values.

2.6 Antibacterial experiments

EC_{50} of the compounds were chosen to present their antibacterial activity. *B. subtilis* was chosen to represent gram-positive bacteria and *E. coli* Rosetta was chosen to represent gram-negative bacteria. For *E. coli*, a single colony was picked to culture in 3 mL fresh LB medium with 100 $\mu\text{g}/\text{mL}$ chloramphenicol overnight at 37 $^{\circ}\text{C}$ with shaking at 190 rpm. For *B. subtilis*, a single colony was picked to culture in 3 mL fresh LB medium overnight at 37 $^{\circ}\text{C}$ with shaking at 190 rpm. The overnight culture was diluted 100-fold into fresh LB medium and incubated 3 h at 37 $^{\circ}\text{C}$ with shaking at 190 rpm. Then, the 3 h culture was diluted 400-fold into fresh LB medium and added with 60 μL of different concentrations of compound **2d** dissolved in 100 % DMSO. After

incubation for 16-20 h at 37 °C with shaking at 190 rpm, their OD₆₀₀ values were measured by Hybrid Multi-Mode Reader.



2.7 Docking compound in *SaUPPS*

The molecular docking was performed using the iGemDOCK to predict how *SaUPPS* interacts with compound **2d**. Compound **2d** was docked to the structures of *SaUPPS* with FPP (PDB ID 4H8E²⁴). Then, the docking results were analyzed to study the interaction between *SaUPPS* and compound **2d** and compare with the interaction between *SaUPPS* and FPP.



3 RESULT

3.1 Synthesis of pyrrolidinone derivatives

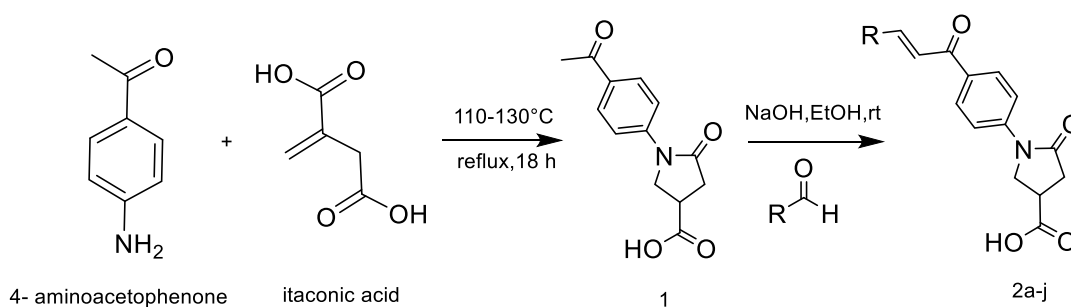
3.1.1 1-(4-Acetylphenyl)-4-carboxy-2-pyrrolidinone (1)

In the beginning, I adopted the method of Ausra et al. reported in 2007³⁵ to synthesize compound **1**. In this method, compound **1** should precipitate in water after adding aq HCl to pH1, but I did not get the same result. Then, I changed the approach to synthesize compound **1**. To prevent compound **1** from dissolving in water, the mixture was heated to melt and reacted themselves without water. Products were dissolved in methanol with heat after reactions and cooled to be recrystallized. Although some products remained in methanol, this approach could be used to get purified compound **1**.

3.1.2 4-Carboxy-1-(4-styrylcarbonylphenyl)-2-pyrrolidinones derivatives (2a-j)

The synthesis of compound **2a-j** was based on aldol condensation, but the synthesis at room temperature for overnight failed to produce products when compound **1** reacted with NaOH and benzaldehyde at the same time. I then added NaOH to deprotonate compound **1** 30 min before adding various benzaldehydes to successfully make compound **2a-j**. Although compound **2a-j** are hydrophobic, they could be dissolved in ddH₂O with aq NaOH because of their carboxyl group. On the other hand, benzaldehydes could be dissolved in EA, but not in ddH₂O. Based on these different

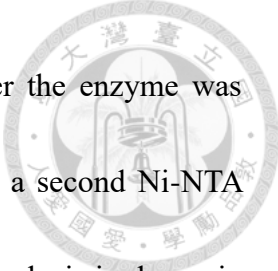
properties, compound **2a-j** were separated from the unreacted benzaldehydes with EA and water by the separatory funnel. Then, the collection of aqueous layers was added HCl to protonate the carboxylate anion, so compounds **2a-j** were precipitated and filtered out. The total synthetic scheme is shown in Scheme 1. Although this method could yield purified compound **2a-j**, it could not be used to yield the compounds with hydrophilic groups. For example, the compound with the hydroxyl group did not precipitate even after adding aq HCl to pH < 1.



Scheme 1. Synthesis of the pyrrolidinone derivatives

3.2 Purification of UPPS

We chose the UPPS in *E. coli* and *S. aureus* to represent gram-negative and gram-positive bacteria, respectively. The plasmid for His-tagged *EcUPPS* has been previously constructed in our laboratory. I cloned the gene of *SaUPPS* into pET32Xa/LIC vector to form the plasmid. Then, the plasmids were transformed in *E. coli* BL21 (*DE3*) to overexpress UPPS. After the first purification step with Ni-NTA column, Factor Xa was added to cleave the His-tag. However, the FXa cleavage




efficiency was quite low, so I cleaved the tag with thrombin. After the enzyme was successfully cleaved by thrombin; UPPS were further purified with a second Ni-NTA column and were collected in flow through. The 10 % SDS-PAGE analysis is shown in figure 2. In this figure, the *Ec*UPPS and *Sa*UPPS with His-tag both had a band close to 48 kDa. After adding thrombin, 15 kDa His-tag and other residues were cut. The finally purified *Ec*UPPS and *Sa*UPPS without His-tag both had a band between 28-35 kDa. These results were consistent with the theoretical values.

3.3 Kinetic constant of UPPS

Because our compounds had absorption at 360 nm which is the detective wavelength in EnzChek pyrophosphate assay kit, MANT-O-GPP was chosen to measure the activity of UPPS. When MANT-O-GPP reacted with IPP to undergo chain elongation by *Ec*UPPS or *Sa*UPPS, its emission at 420 nm increased. The fluorescence change of MANT-O-GPP can be converted to reaction velocity by using its linear standard curve; this method can be used to measure the kinetics of UPPS³³⁻³⁴. The linear standard curve of MANT-O-GPP was determined in Figure 3. As shown in Figure 4 and 5, the K_m of MANT-O-GPP and IPP were 0.67 and 24.33 μ M, respectively, for *Ec*UPPS. The K_m of MANT-O-GPP and IPP were 0.32 and 0.38 μ M, respectively, for *Sa*UPPS. *Sa*UPPS had higher k_{cat} than *Ec*UPPS (Table 1).

3.4 Compound 2a-j inhibit UPPS activity



To test the inhibition of compound **2a-j** on UPPS, we added different concentrations of compound **2a-j** to IPP and MANT-O-GPP in the concentrations of their K_m . The compound **VK-278** was also tested with the same method (Figure 6, 7). Their IC_{50} values are shown in Table 2. According to these results, we could get there conclusions. First, the compounds with halogen and benzene group were more potent to inhibit the activity of UPPS. Compounds **2b-d** with halogen more easily enter the activity site of UPPS due to their higher inductive effects and lower steric hindrance. On the other hand, the compound **2i** with benzene group and FPP the substrate of UPPS both were hydrophobic, so the compound **2i** was more suitable in the active site of UPPS. Second, comparing compound **2f** to **2g** or **VK-278** to **2h**, we found that the positions of substituents affected their inhibition. The para-substituted compounds were more potent to inhibit the activity of UPPS than the meta-substituted compounds. Third, based on the properties of halogen, we tried to synthesize the compound with more halogen. Compound **2j** having two chlorines were the most potent to inhibit the activity of UPPS and had low micromolar IC_{50} value.



3.5 Antibacterial activity of compound **2d**, **i**, **j**

To test whether these compounds could inhibit the growth of bacteria, their EC_{50} values were measured. Three of compounds were displaying more potent to inhibit the activity of UPPS were tested on *E. coli* first. Although these compounds could be dissolved in DMSO, they had to be added into LB medium. Since the survival of *E. coli* was little affected by 2 % DMSO³⁶, these compounds were dissolved in LB medium with 2% DMSO as the final concentration. Under this situation, the maximum concentration of the compounds was 800 μ M. After treating each compound overnight, *E. coli* grew well as the control without the compound. *E. coli* was one of the gram-negative bacteria which had the outer membrane, so these compounds were difficult to cross the cell wall³⁷. Then, we tested whether these compounds could inhibit gram-positive bacteria. Due to the biosafety Level of *S. aureus*, we chose *B. subtilis* to represent the gram- positive bacteria. Compound **2d** in 800 μ M and compound **2i**, **2j** in 400 μ M could inhibit over 90 % *B. subtilis* growth (Figure 8). The values of EC_{50} are listed in Table 3. These results show that these compounds could inhibit the growth of *B. subtilis*, so they may also inhibit the growth of other gram-positive bacteria. In addition, we could find that Compound **2i** has more potential to inhibit the growth of *B. subtilis* than compound **2j** which was opposite to IC_{50} values. This unexpected result may due to the hydrophobic of compound **2i** which makes it cross cell membrane easier.



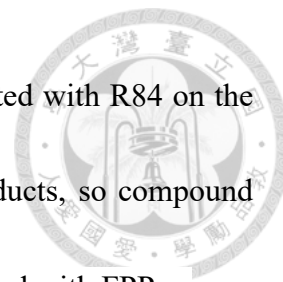
3.6 Compound 2d was a mixed inhibitor

To investigate the inhibition types of these compounds, we chose compound **2d** which had better yield during synthesis and more potent to inhibit UPPS activity to react with different concentrations of substrates. The lineweaver-burk plot shown in Figure 9 revealed mixed inhibition pattern (three lines intersect at the second quadrant and close to the y-axis) against *Sa*UPPS with respect to both IPP and MANT-O-GPP. Based on these results, compound **2d** was supposed to bind at a different location from those for binding of IPP and MANT-O-GPP. Based on this result, the values of K_i of IPP and MANT-O-GPP were determined as 29.0 ± 1.8 and 30.2 ± 1.5 μM , respectively. Then, the values of K_i' of IPP and MANT-O-GPP were determined as 26.5 ± 7.1 and 34.5 ± 8.7 μM , respectively.

3.7 Compound 2d docked in the activity site of UPPS with FPP

To predict the compound binding location, iGEMDOCK computer program was used to dock compound **2d** and UPPS containing FPP. The best docking results are shown in Figure 10. Although compound **2d** seemed to be docked in the active site of UPPS, the residues interacting with compound **2d** were different from those with FPP. The compound **2d** did not interact with the p-loop (G-N-G-R motif) which is used to recognize FPP and catalysis (D33 in *Sa*UPPS)³⁸⁻³⁹, confirming its non-competition in

binding. On the other hand, the compound **2d** and FPP both interacted with R84 on the loop (F77-R84) which controls channel opening to release the products, so compound **2d** could bind to the UPPS whether or not the UPPS has already bound with FPP.



4 DISCUSSION



UPPS catalyzes the condensation of IPP and FPP to form UPP which is a carrier for peptidoglycans synthesis, so it is a key enzyme for the synthesis of bacterial cell wall¹⁹. Because of its role, UPPS could be a valid target for antibiotic²³⁻²⁸. In fact, it has been postulated that several antibiotics without known targets may inhibit UPPS^{25, 37}. Therefore, we designed and synthesized a series of 1-(4-Acetylphenyl)-4-carboxy-2-pyrrolidinone derivatives to inhibit the activity of UPPS and thus the growth of bacteria.

We tried to mainly synthesize the derivatives with electron-withdrawing substituents on the benzaldehydes. Compound **2a-j** were synthesized successfully. Using the same approach, we intended to synthesize the compounds with electron-donating groups such as 4-diethylaminobenzaldehyde but the products were either with low yield or impure. We also tried to use other aldehydes to replace benzaldehydes, but the products were also impure and difficult to be purified by precipitation. Therefore, the approach still requires modification.

Although the EnzChek pyrophosphate assay kit was commonly used to assay the activity of UPPS^{27, 40}, our compound had absorbance at 360 nm, the same as the detected wavelength in this assay. The other assay method by using [¹⁴C]IPP to monitor the activity^{16, 33, 41} is tedious and expensive. As a result, we used MANT-O-GPP which

was an analog of FPP with fluorescence to evaluate the activity of UPPS³³⁻³⁴. Before measuring the IC₅₀ values of compounds, the K_m of UPPS had to be determined.

Although the K_m value of IPP for *Sa*UPPS was different from reported probably due to the different substrates used. Based on the K_m of IPP and MANT-O-GPP, we used those concentrations to measure the IC₅₀ of compounds. According to the inhibition assay, compound **2d**, **2i**, **2j**, and **2k** were more potent to inhibit UPPS activity. Compound **2d** and **2j** with halogens have inductive effects and low steric hindrance, so their structures suited to the active site of UPPS. Then, compound **2j** was more potent to inhibit UPPS because it had one more halogen on benzene to withdraw electrons. On the other hand, compound **2i** was highly hydrophobic like FPP, so it could fit into the active site of UPPS. These compounds had low micromolar ranges of IC₅₀, so they may have the potential to inhibit the growth of bacteria.

To investigate the antibacterial activity of these compounds, we test their EC₅₀ values for *E. coli* and *B. subtilis*. The EC₅₀ values of compound **2d**, **2i**, and **2j** for *E. coli* were too high to be determined probably because of the thick cell wall of *E. coli*. This situation was beneficial to the treatment for *S. aureus* because most of *E. coli* were good for human bodies. Due to the high risk of growing *S. aureus*, we chose *B. subtilis* and the EC₅₀ values of compound **2d**, **2i**, and **2j** were approximately 100-300 μM, higher than the IC₅₀ values in inhibiting UPPS. The inefficiency may be due to the difficulty of

the compounds across the cell wall, which needs to be further tested. Moreover, their solubility in water can be improved by using various acids to solify them³⁷.

Based on the results of the inhibition and the docking experiments, we assume that these compound were the mixed-type or non-competitive type of inhibitors against UPPS. But the docking models were speculations, they might not be correct. However, the actual interactions between the compounds and UPPS have to be ensured by crystallographic structural studies.

In conclusion, although the antibacterial activities of the tested compounds were not good enough for the treatment of bacterial infectious diseases, they were effective to inhibit UPPS activity with low micromolar IC_{50} . This series of compounds could serve as a starting point for a new class of antibiotics after optimization.

TABLE**Table 1. The kinetic constants of *Ec*UPPS and *Sa*UPPS.**

Protein	MANT-O-GPP K_m (μM)	IPP K_m (μM)	k_{cat} (s^{-1})
<i>Ec</i> UPPS	0.67 ± 0.077	24.33 ± 3.33	0.020 ± 0.001
<i>Sa</i> UPPS	0.31 ± 0.03	0.41 ± 0.04	0.085 ± 0.002

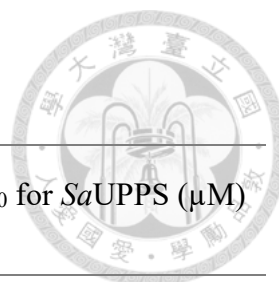


Table 2. The IC₅₀ of compounds against *Ec*UPPS and *Sa*UPPS.

Compound	R group	IC ₅₀ for <i>Ec</i> UPPS (μM)	IC ₅₀ for <i>Sa</i> UPPS (μM)
2a	phenyl	34.7 ± 1.0	55.5 ± 1.0
2b	4-fluorophenyl	22.5 ± 1.0	27.2 ± 1.1
2c	4-chlorophenyl	16.7 ± 1.0	17.9 ± 1.1
2d	4-bromophenyl	10.8 ± 1.1	15.5 ± 1.0
2e	4-carboxyphenyl	63.5 ± 1.1	88.4 ± 1.0
2f	4-cyanophenyl	32.1 ± 1.0	39.3 ± 1.1
2g	3-cyanophenyl	51.9 ± 1.0	70.2 ± 1.0
VK-278	4-nitrophenyl	12.7 ± 1.0	20.1 ± 1.1
2h	3-nitrophenyl	36.2 ± 1.0	41.3 ± 1.1
2i	biphenyl	4.4 ± 1.1	5.0 ± 1.0
2j	3,4-dichlorophenyl	1.7 ± 1.0	6.4 ± 1.0
2k	furanyl	11.0 ± 1.0	18.7 ± 1.0

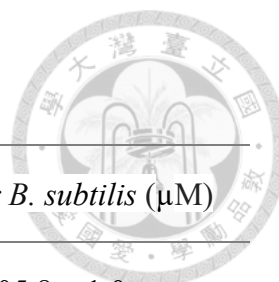


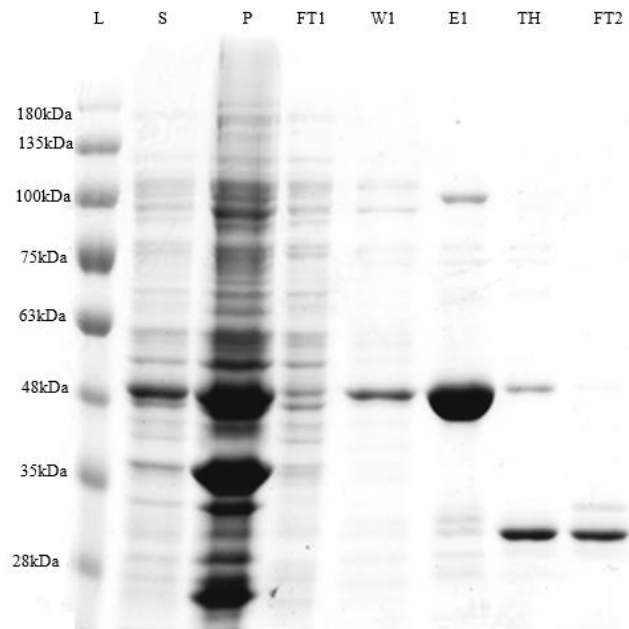
Table 3. The EC₅₀ values of compound 2d, i, and j.

Compound	EC ₅₀ for <i>E. coli</i> (μM)	EC ₅₀ for <i>B. subtilis</i> (μM)
2d	> 800	305.8 ± 1.0
2i	> 800	109.1 ± 1.1
2j	> 800	208.9 ± 1.1



FIGURE

(A)



(B)

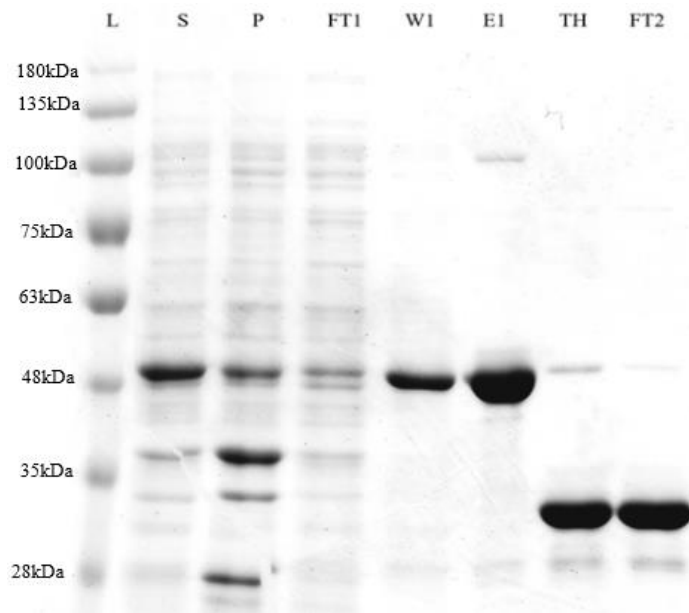


Figure 2. SDS-PAGE analysis of the purified *Ec*UPPS and *Sa*UPPS.

(A) SDS-PAGE analysis of *Ec*UPPS after different steps of purification. (B) SDS-PAGE analysis of *Sa*UPPS after different steps of purification. L: prestained protein ladder; S: Supernatant; P: Pallet; FT1: flow through with 10 mM imidazole buffer from the first Ni-NTA column; W1 : washed with 25 mM imidazole; E1: eluted with 250 mM imidazole; TH : E1 treated with Thrombin at 4°C overnight; FT2 : TH pass Ni-NTA column;

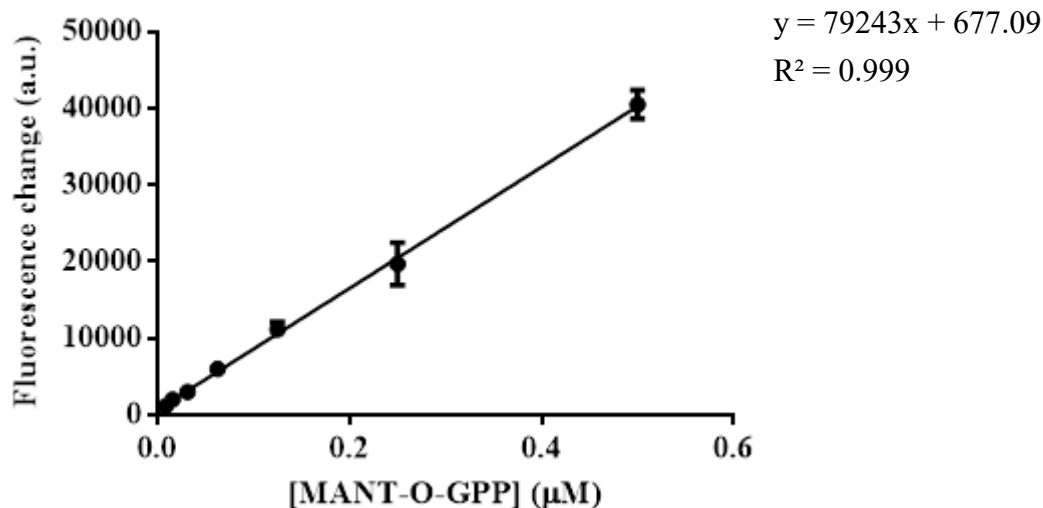


Figure 3. The linear standard curve of MANT-O-GPP converts to the product.

The plot of the total fluorescence change vs. the different concentrations of MANT-O-GPP used for converting to product catalyzed by 0.01 µM of UPPS 10mins. The extinction coefficient of MANT-O-GPP converted to the product was determined to be 79243 a.u./1 µM (the slope of the fitted line). The conversion was assumed to be 100%.

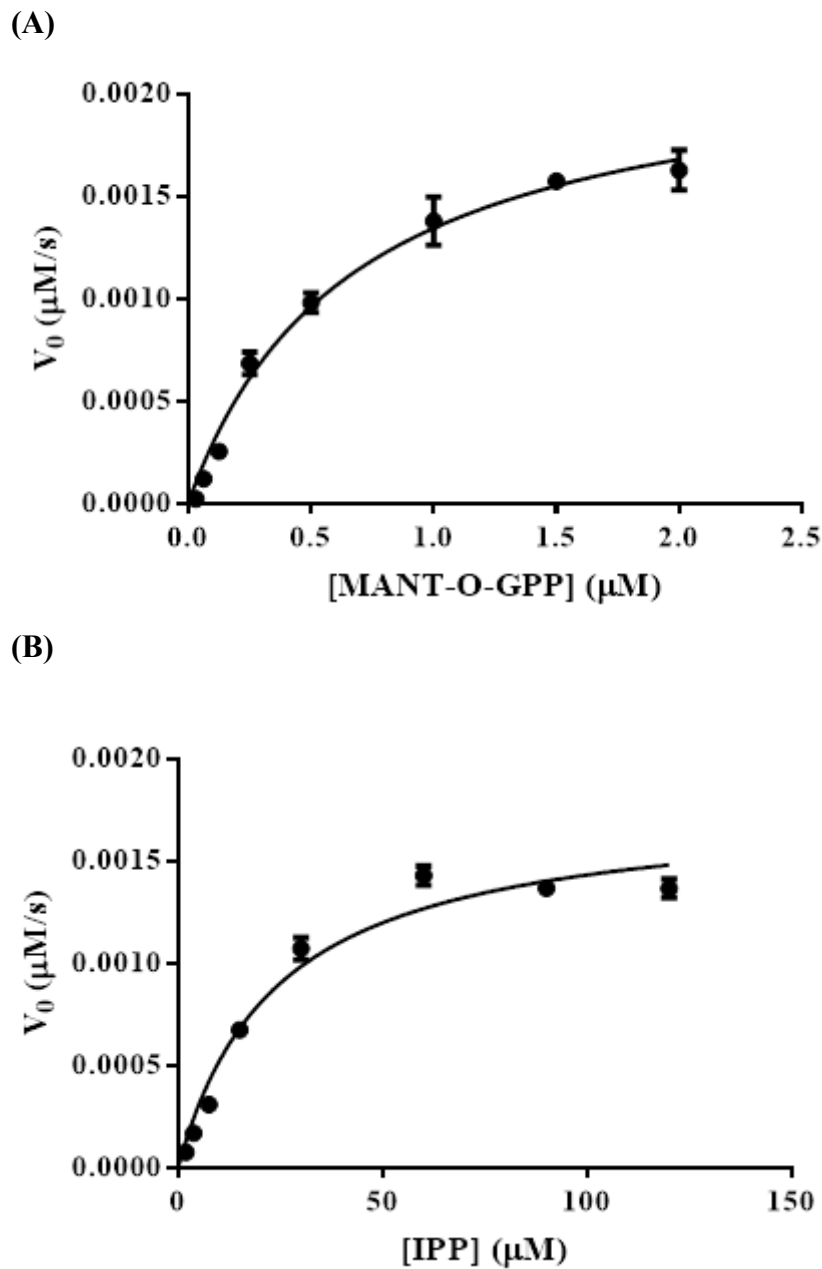
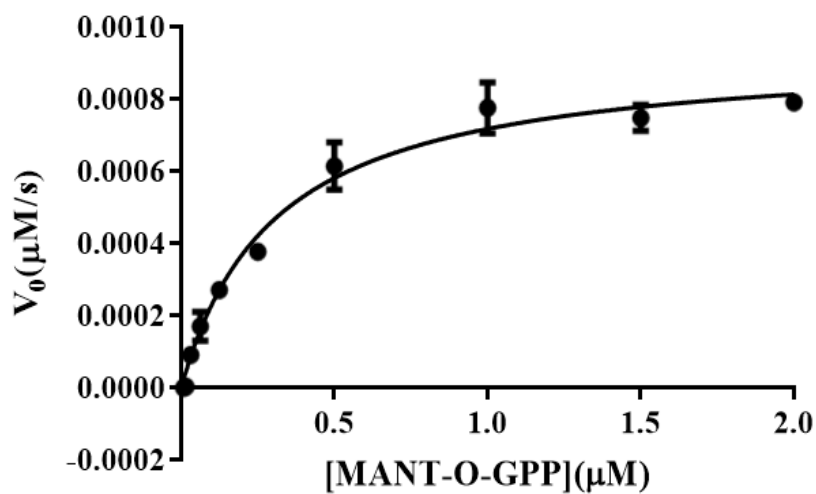


Figure 4. The kinetic constant of *EcUPPS*.

(A) The plot of V_0 vs. [MANT-O-GPP] was fitted with Michaelis-Menten equation to yield the K_m of MANT-O-GPP and k_{cat} of *EcUPPS*. (B) The plot of V_0 vs. [IPP] for the K_m of IPP and k_{cat} of *EcUPPS*.



(A)



(B)

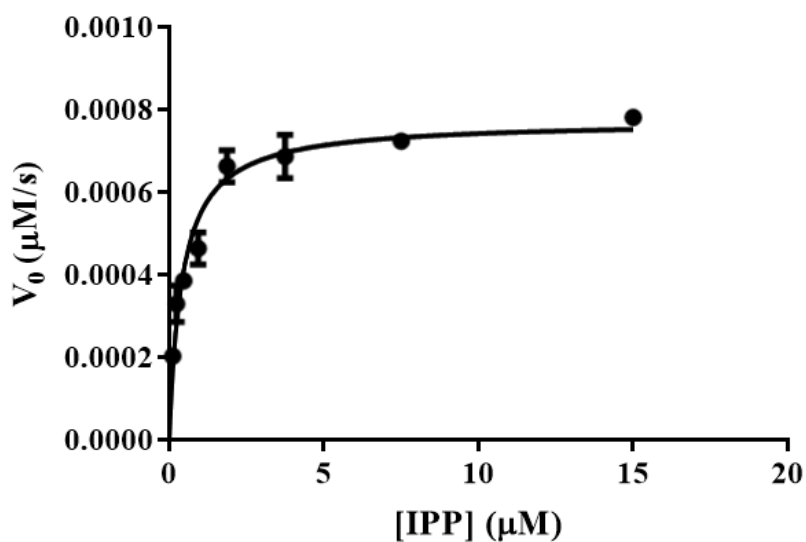
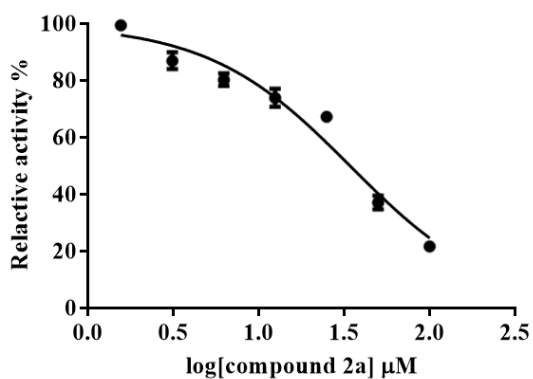


Figure 5. The kinetic constant of *Sa*UPPS.

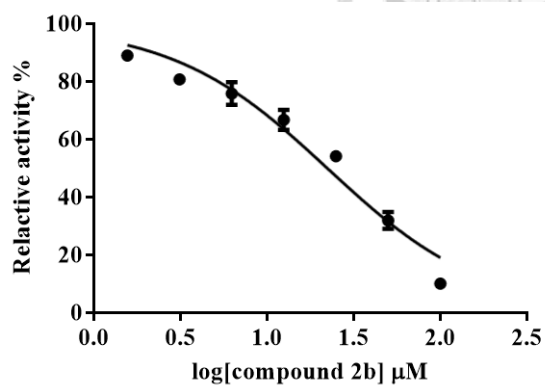
(A) The plot of V_0 vs. [MANT-O-GPP] was fitted with Michaelis-Menten equation to yield the K_m of MANT-O-GPP and k_{cat} of *Ec*UPPS. (B) The plot of V_0 vs. [IPP] for the K_m of IPP and k_{cat} of *Ec*UPPS.



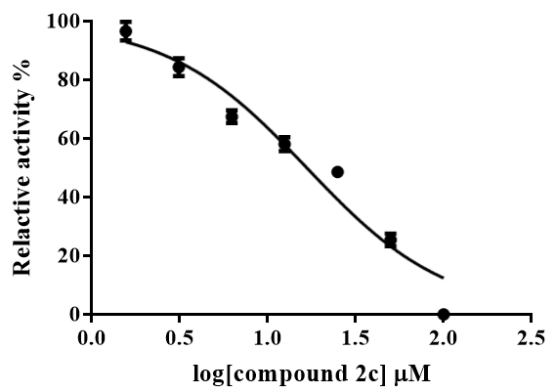
(A)



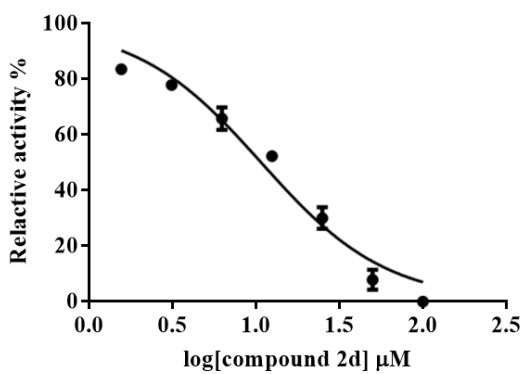
(B)



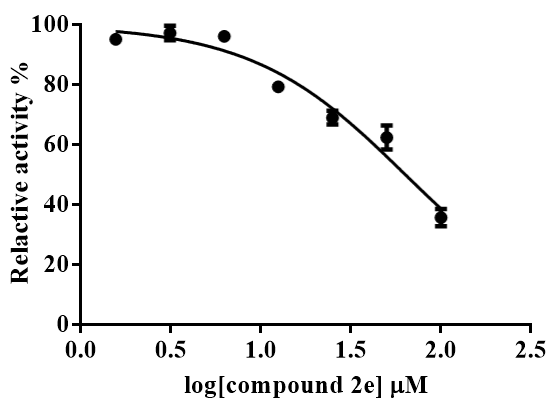
(C)



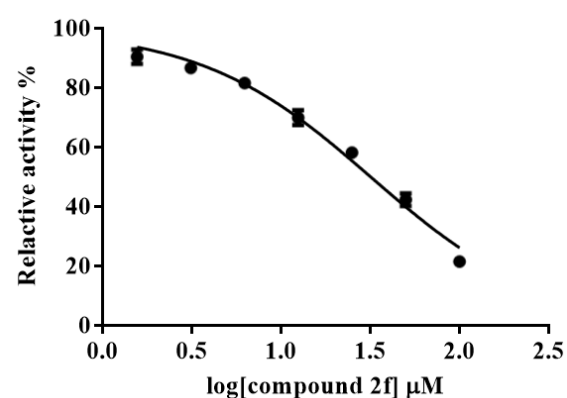
(D)



(E)

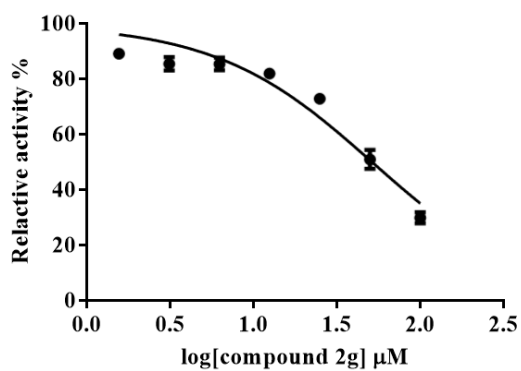


(F)

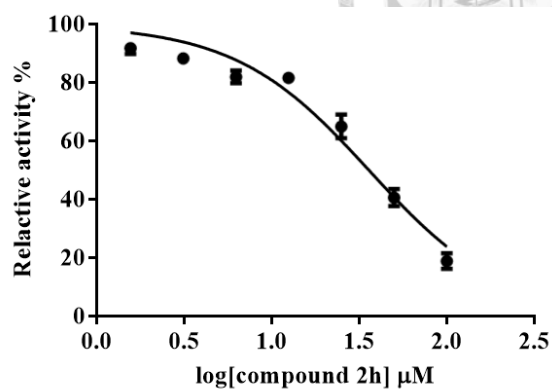




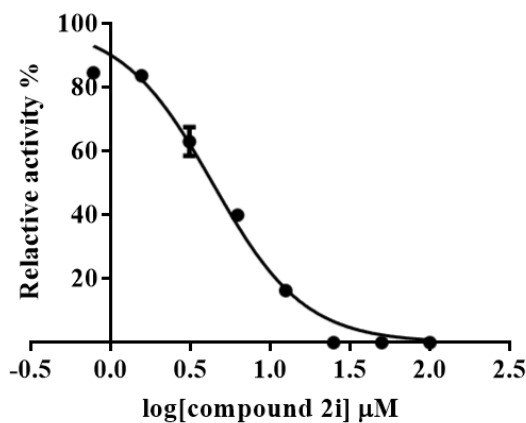
(G)



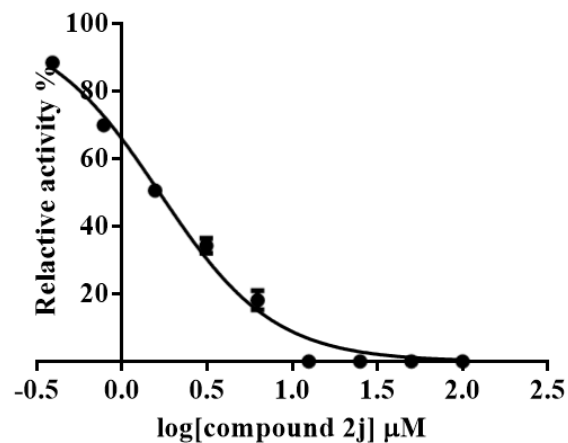
(H)



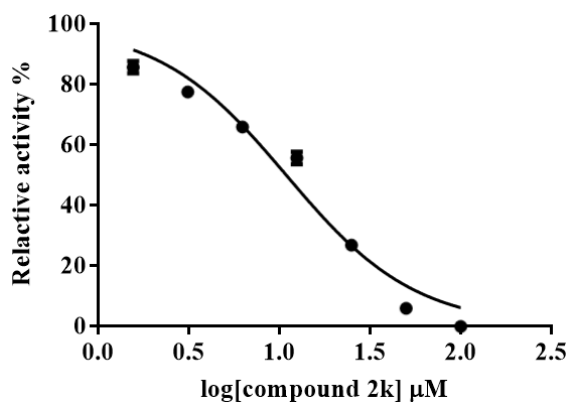
(I)



(J)



(K)



(L)

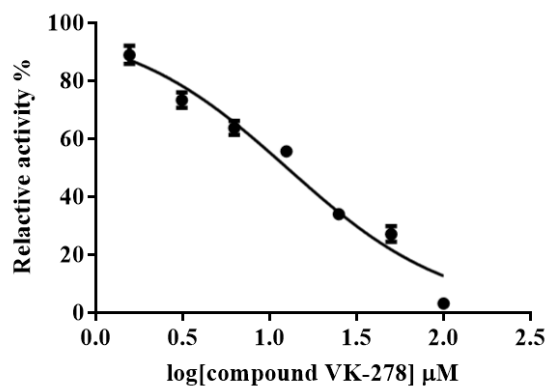
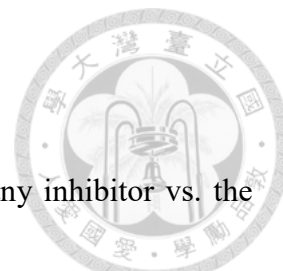


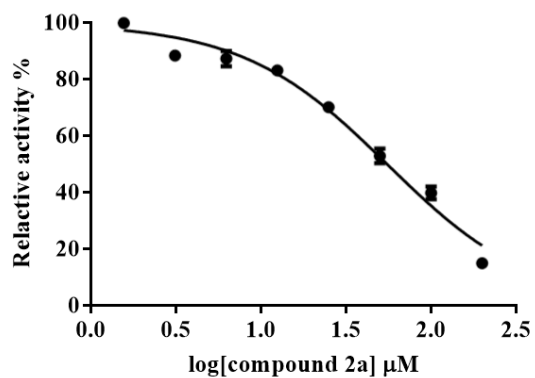
Figure 6. The inhibition assay for *EcUPPS*.

These plots are *EcUPPS* activities relative to the control without any inhibitor vs. the logarithm values of compound concentrations for (A) **2a**, (B) **2b**, (C) **2c**, (D) **2d**, (E) **2e**, (F) **2f**, (G) **2g**, (H) **2h**, (I) **2i**, (J) **2j**, (K) **2k**, and (L) **VK-278**.

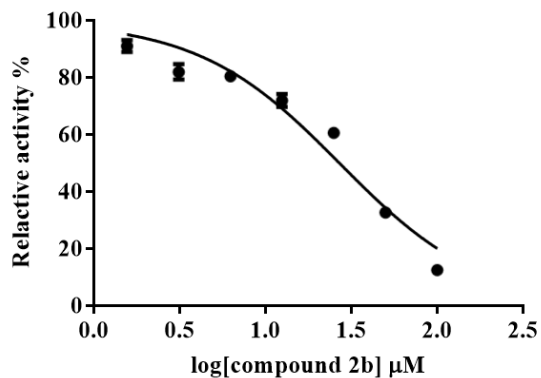




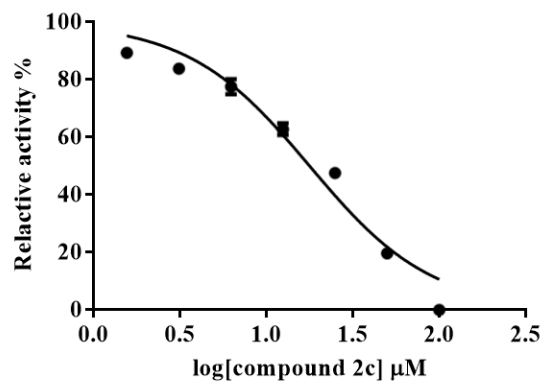
(A)



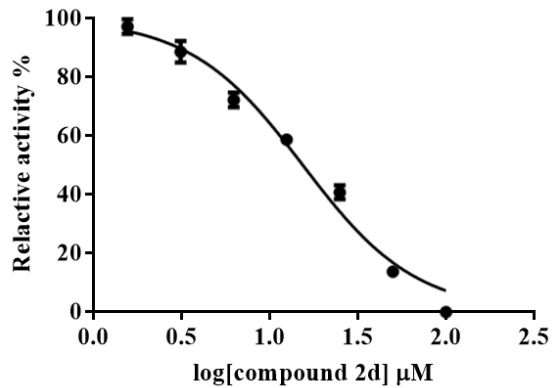
(B)



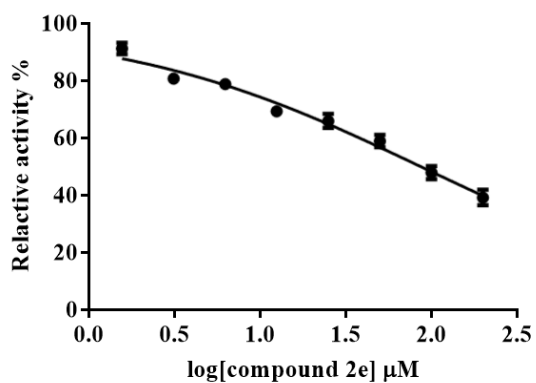
(C)



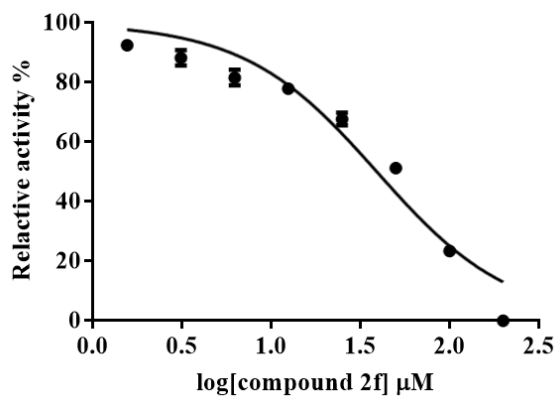
(D)



(E)

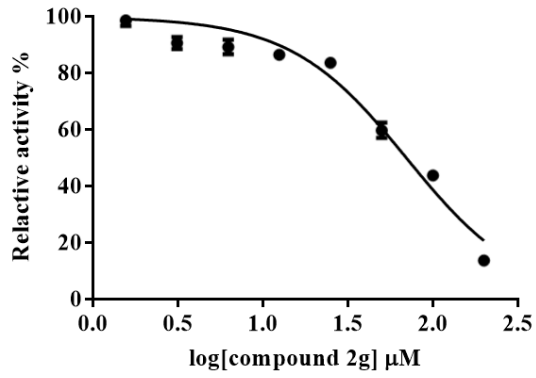


(F)

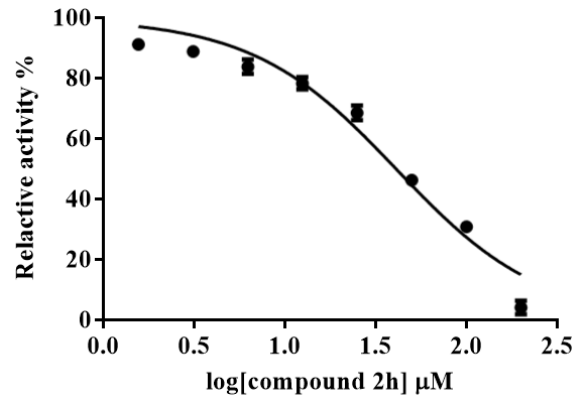




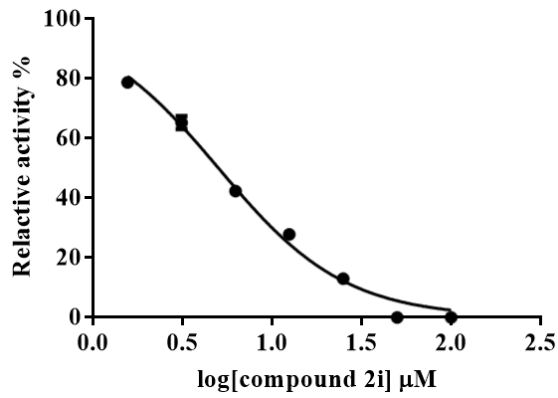
(G)



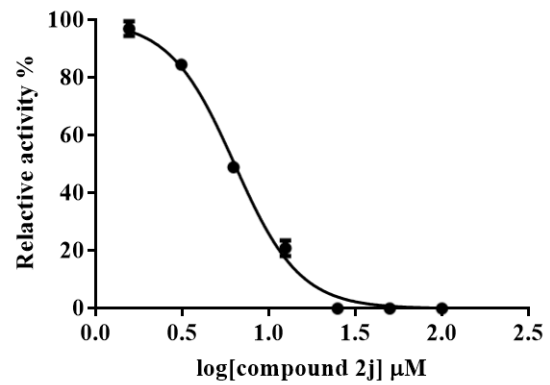
(H)



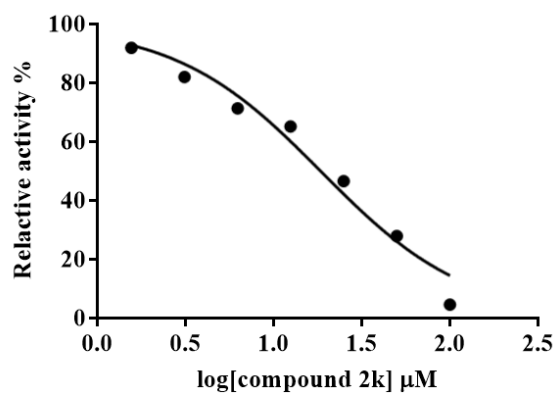
(I)



(J)



(K)



(L)

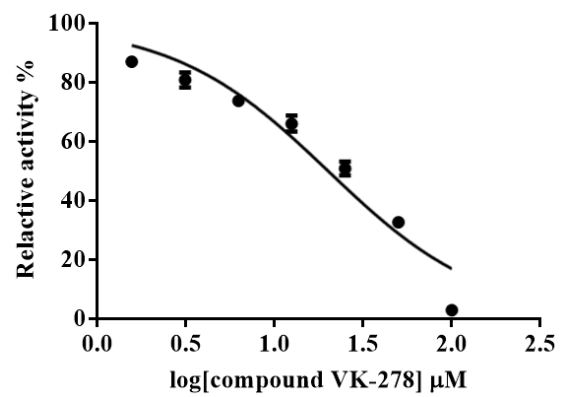
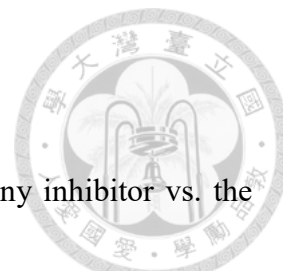


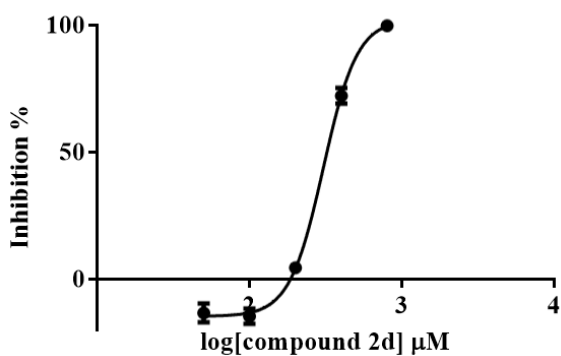
Figure 7. The inhibition assay for *Sa*UPPS.

These plots are *Sa*UPPS activities relative to the control without any inhibitor vs. the logarithm values of compound concentrations for (A) **2a**, (B) **2b**, (C) **2c**, (D) **2d**, (E) **2e**, (F) **2f**, (G) **2g**, (H) **2h**, (I) **2i**, (J) **2j**, (K) **2k**, and (L) **VK-278**.

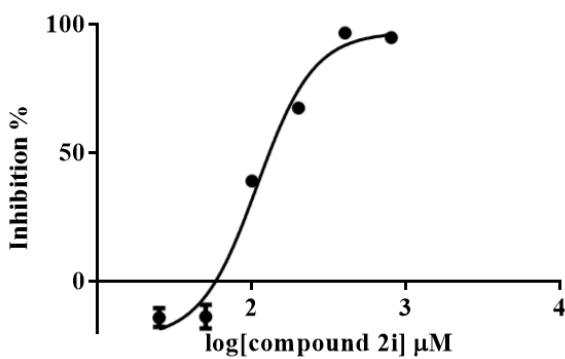




(A)



(B)



(C)

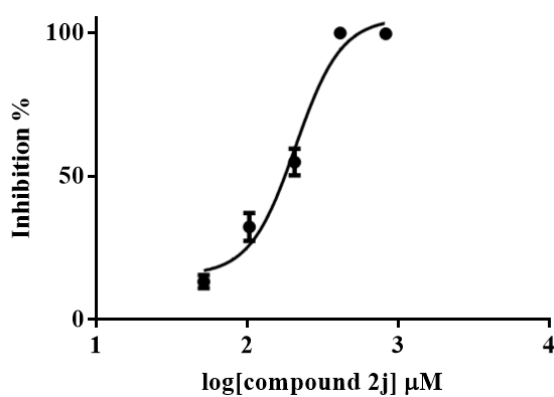


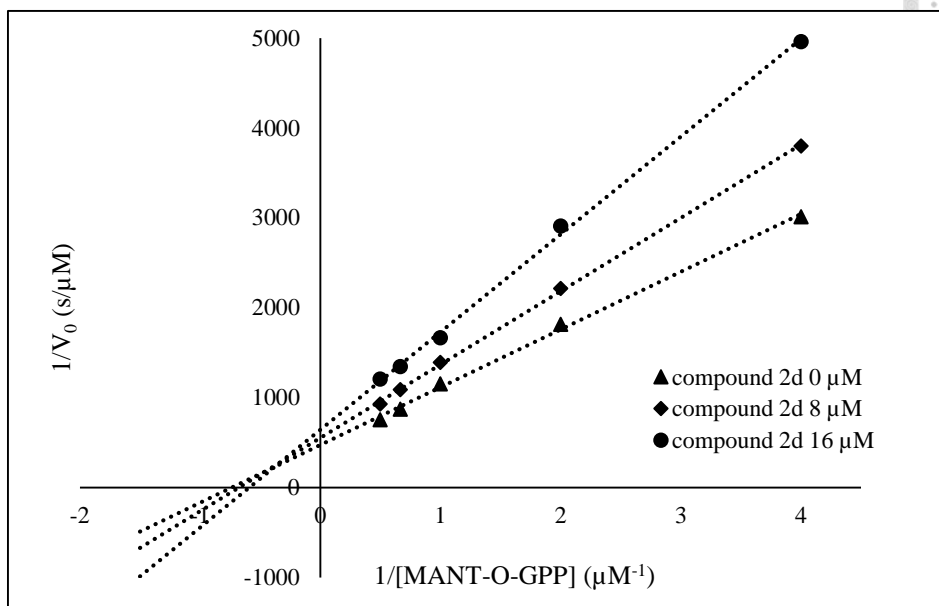
Figure 8. The EC₅₀ of compound 2d, I and j against *B. subtilis*.

These plots are cell numbers relative to the control without any inhibitor vs. the

logarithm of compound concentrations for (A) 2d, (B) 2i, and (C) 2j.



(A)



(B)

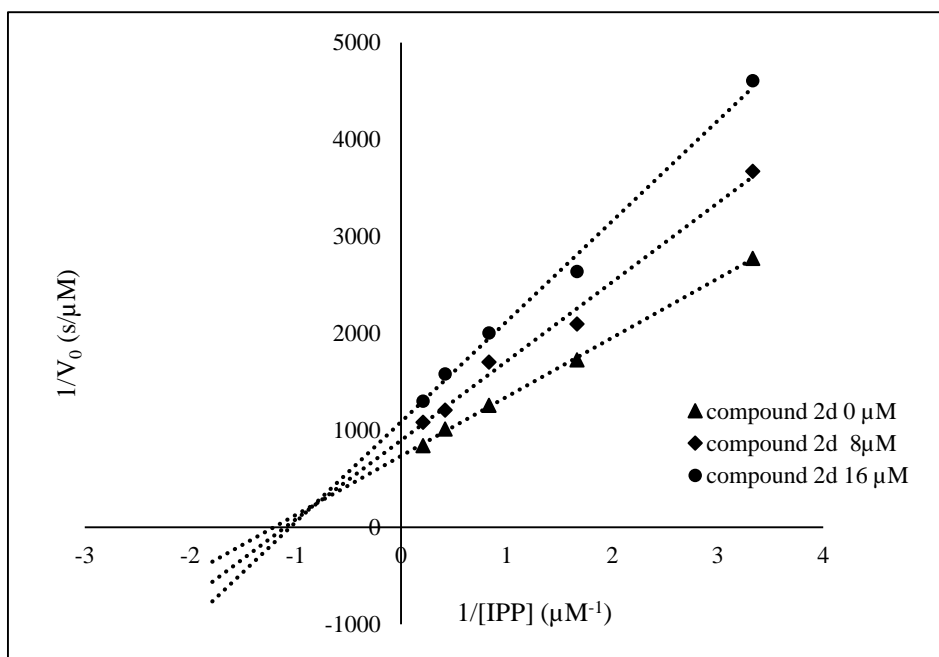


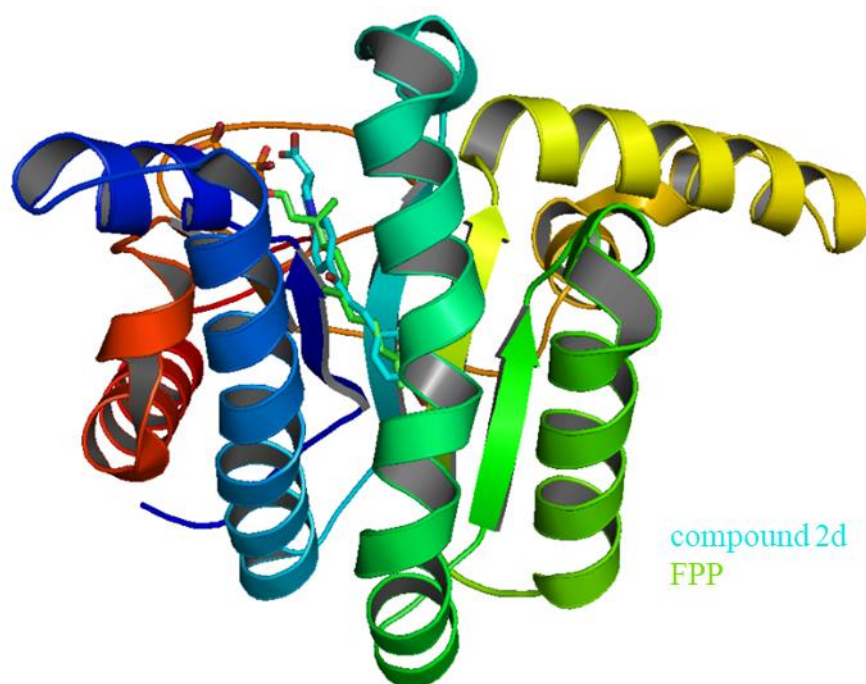
Figure 9. Compound 2d is a mixed inhibitor of *Sa*UPPS.

The lineweaver-burk plots of *Sa*UPPS $1/V_0$ vs. $1/[MANT-O-GPP]$ (A) and $1/[IPP]$ (B)

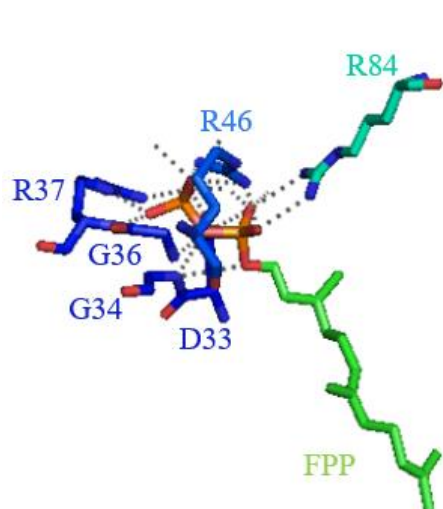
for compound **2d**.



(A)



(B)



(C)

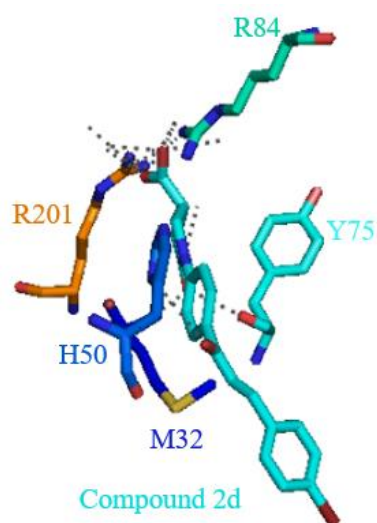


Figure 10. Docking of compound 2d in *SaUPPS* with FPP.

(A) The docking model of compound **2d** in *SaUPPS* with FPP.

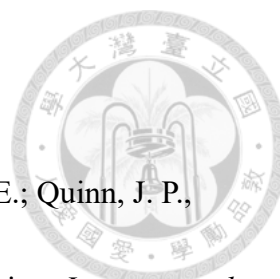
(B) The interactions between *SaUPPS* and FPP.

(C) The interactions between *SaUPPS* and compound **2d**.



REFERENCE

1. Arturo Casadevall, L.-a. P., Microbiology: Ditch the term pathogen. *Nature News* **2014**.
2. Smith, I., Mycobacterium tuberculosis pathogenesis and molecular determinants of virulence. *Clin Microbiol Rev* **2003**, *16* (3), 463-496.
3. Scallan, E.; Hoekstra, R. M.; Angulo, F. J.; Tauxe, R. V.; Widdowson, M.-A.; Roy, S. L.; Jones, J. L.; Griffin, P. M., Foodborne illness acquired in the United States--major pathogens. *Emerg Infect Dis* **2011**, *17* (1), 7-15.
4. Wilhelm, S., Pneumonia. In *xPharm: The Comprehensive Pharmacology Reference*, Enna, S. J.; Bylund, D. B., Eds. Elsevier: New York, **2007**; pp 1-6.
5. Prasad, G.; Dahiya, S., *Study of the general characteristics of disease caused by bacteria, viruses, fungi and protozoa*. **2019**.
6. Fleming, A., On the antibacterial action of cultures of a penicillium, with special reference to their use in the isolation of *B. influenzae*. 1929. *Bulletin of the World Health Organization* **2001**, *79* (8), 780-790.
7. R. R. Yocum, J. R. R., J. L. Strominger, The mechanism of action of penicillin. Penicillin acylates the active site of *Bacillus stearothermophilus* D-alanine carboxypeptidase. *J Biol Chem*. **1980**, *255*(9): 3977–3986.
8. Newsom, S. W. B., MRSA--past, present, future. *Journal of the Royal Society of*



Medicine **2004**, *97* (11), 509-510.

9. Bradley, J. S.; Garau, J.; Lode, H.; Rolston, K. V. I.; Wilson, S. E.; Quinn, J. P.,

Carbapenems in clinical practice: a guide to their use in serious infection. *International*

Journal of Antimicrobial Agents **1999**, *11* (2), 93-100.

10. Neu, H. C., The Crisis in Antibiotic Resistance. *Science* **1992**, *257* (5073),

1064-1073.

11. Rice, L. B., Federal Funding for the Study of Antimicrobial Resistance in

Nosocomial Pathogens: No ESKAPE. *The Journal of Infectious Diseases* **2008**, *197* (8),

1079-1081.

12. Livermore, D. M., Linezolid in vitro : mechanism and antibacterial spectrum.

Journal of Antimicrobial Chemotherapy **2003**, *51* (suppl_2), ii9-ii16.

13. Wang, Y.; Desai, J.; Zhang, Y.; Malwal, S. R.; Shin, C. J.; Feng, X.; Sun, H.; Liu,

G.; Guo, R.-T.; Oldfield, E., Bacterial Cell Growth Inhibitors Targeting Undecaprenyl

Diphosphate Synthase and Undecaprenyl Diphosphate Phosphatase. *ChemMedChem*

2016, *11* (20), 2311-2319.

14. Parmar, A.; Lakshminarayanan, R.; Iyer, A.; Mayandi, V.; Leng Goh, E. T.; Lloyd,

D. G.; Chalasani, M. L. S.; Verma, N. K.; Prior, S. H.; Beuerman, R. W.; Madder, A.;

Taylor, E. J.; Singh, I., Design and Syntheses of Highly Potent Teixobactin Analogues

against *Staphylococcus aureus*, Methicillin-Resistant *Staphylococcus aureus* (MRSA),



and Vancomycin-Resistant Enterococci (VRE) in Vitro and in Vivo. *Journal of Medicinal Chemistry* **2018**, 61 (5), 2009-2017.

15. El Ghachi, M.; Howe, N.; Huang, C.-Y.; Olieric, V.; Warshamanage, R.; Touzé, T.; Weichert, D.; Stansfeld, P. J.; Wang, M.; Kerff, F.; Caffrey, M., Crystal structure of undecaprenyl-pyrophosphate phosphatase and its role in peptidoglycan biosynthesis. *Nature Communications* **2018**, 9 (1), Article number : 1078.

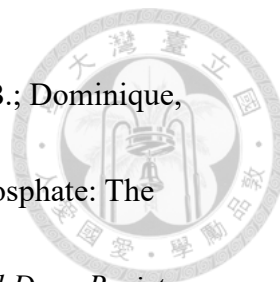
16. Durrant, J. D.; Cao, R.; Gorfe, A. A.; Zhu, W.; Li, J.; Sankovsky, A.; Oldfield, E.; McCammon, J. A., Non-bisphosphonate inhibitors of isoprenoid biosynthesis identified via computer-aided drug design. *Chemical biology & drug design* **2011**, 78 (3), 323-332.

17. Gautam, A.; Rishi, P.; Tewari, R., UDP-N-acetylglucosamine enolpyruvyl transferase as a potential target for antibacterial chemotherapy: recent developments. *Applied Microbiology and Biotechnology* **2011**, 92 (2), 211.

18. Liang, P.-H.; Ko, T.-P.; Wang, A. H.-J., Structure, mechanism and function of prenyltransferases. *European Journal of Biochemistry* **2002**, 269 (14), 3339-3354.

19. Robyt, J., *Essentials of Carbohydrate Chemistry*. Springer Verlag, New York: **1998**; Vol. pp. 305–318 (Chapter 10).

20. Ogura, K.; Koyama, T., Enzymatic Aspects of Isoprenoid Chain Elongation. *Chemical Reviews* **1998**, 98 (4), 1263-1276.



21. Guillaume, M.; Sophie, R.; Rodolphe, A.; Ahmed, B.; Hélène, B.; Dominique, M.-L.; Thierry, T., Deciphering the Metabolism of Undecaprenyl-Phosphate: The Bacterial Cell-Wall Unit Carrier at the Membrane Frontier. *Microbial Drug Resistance* **2014**, *20* (3), 199-214.
22. Marko Jukič, K. R. a. S. G., Recent Advances in the Development of Undecaprenyl Pyrophosphate Synthase Inhibitors as Potential Antibacterials. *Current Medicinal Chemistry* **2016**, *23* (5), 464-482.
23. Teng, K.-H.; Liang, P.-H., Structures, mechanisms and inhibitors of undecaprenyl diphosphate synthase: A cis-prenyltransferase for bacterial peptidoglycan biosynthesis. *Bioorganic Chemistry* **2012**, *43*, 51-57.
24. Zhu, W.; Zhang, Y.; Sinko, W.; Hensler, M. E.; Olson, J.; Molohon, K. J.; Lindert, S.; Cao, R.; Li, K.; Wang, K.; Wang, Y.; Liu, Y.-L.; Sankovsky, A.; de Oliveira, C. A. F.; Mitchell, D. A.; Nizet, V.; McCammon, J. A.; Oldfield, E., Antibacterial drug leads targeting isoprenoid biosynthesis. *Proceedings of the National Academy of Sciences* **2013**, *110* (1), 123-128.
25. Sinko, W.; Wang, Y.; Zhu, W.; Zhang, Y.; Feixas, F.; Cox, C. L.; Mitchell, D. A.; Oldfield, E.; McCammon, J. A., Undecaprenyl Diphosphate Synthase Inhibitors: Antibacterial Drug Leads. *Journal of Medicinal Chemistry* **2014**, *57* (13), 5693-5701.
26. Dodbele, S.; Martinez, C. D.; Troutman, J. M., Species Differences in Alternative



Substrate Utilization by the Antibacterial Target Undecaprenyl Pyrophosphate Synthase.

Biochemistry **2014**, 53 (30), 5042-5050.

27. Czarny, T. L.; Brown, E. D., A Small-Molecule Screening Platform for the

Discovery of Inhibitors of Undecaprenyl Diphosphate Synthase. *ACS Infectious*

Diseases **2016**, 2 (7), 489-499.

28. Concha, N.; Huang, J.; Bai, X.; Benowitz, A.; Brady, P.; Grady, L. C.; Kryn, L. H.;

Holmes, D.; Ingraham, K.; Jin, Q.; Pothier Kaushansky, L.; McCloskey, L.; Messer, J.

A.; O'Keefe, H.; Patel, A.; Satz, A. L.; Sinnamon, R. H.; Schneck, J.; Skinner, S. R.;

Summerfield, J.; Taylor, A.; Taylor, J. D.; Evindar, G.; Stavenger, R. A., Discovery and

Characterization of a Class of Pyrazole Inhibitors of Bacterial Undecaprenyl

Pyrophosphate Synthase. *Journal of Medicinal Chemistry* **2016**, 59 (15), 7299-7304.

29. Kuo, C.-J.; Guo, R.-T.; Lu, I.-L.; Liu, H.-G.; Wu, S.-Y.; Ko, T.-P.; Wang, A. H.-J.;

Liang, P.-H., Structure-Based Inhibitors Exhibit Differential Activities against

Helicobacter pylori and *Escherichia coli* Undecaprenyl Pyrophosphate Synthases.

Journal of Biomedicine and Biotechnology **2008**, 2008, Article ID : 841312.

30. Danley, D. E.; Baima, E. T.; Mansour, M.; Fennell, K. F.; Chrnyk, B. A.; Mueller,

J. P.; Liu, S.; Qiu, X., Discovery and structural characterization of an allosteric inhibitor

of bacterial cis-prenyltransferase. *Protein Science* **2015**, 24 (1), 20-26.

31. Farha, M. A.; Czarny, T. L.; Myers, C. L.; Worrall, L. J.; French, S.; Conrady, D. G.;



Wang, Y.; Oldfield, E.; Strynadka, N. C. J.; Brown, E. D., Antagonism screen for inhibitors of bacterial cell wall biogenesis uncovers an inhibitor of undecaprenyl diphosphate synthase. *Proceedings of the National Academy of Sciences* **2015**, *112* (35), 11048-11053.

32. Inokoshi, J.; Nakamura, Y.; Komada, S.; Komatsu, K.; Umeyama, H.; Tomoda, H., Inhibition of bacterial undecaprenyl pyrophosphate synthase by small fungal molecules. *The Journal Of Antibiotics (Tokyo)* **2016**, *69*, 798-805.

33. Teng, K.-H.; Chen, A. P. C.; Kuo, C.-J.; Li, Y.-C.; Liu, H.-G.; Chen, C.-T.; Liang, P.-H., Fluorescent substrate analog for monitoring chain elongation by undecaprenyl pyrophosphate synthase in real time. *Analytical Biochemistry* **2011**, *417* (1), 136-141.

34. Teng, K.-H.; Hsu, E.-T.; Chang, Y.-H.; Lin, S.-W.; Liang, P.-H., Fluorescent Farnesyl Diphosphate Analogue: A Probe To Validate trans-Prenyltransferase Inhibitors. *Biochemistry* **2016**, *55* (31), 4366-4374.

35. Voskiene, A.; Mickevicius, V.; Mikulskiene, G., *Synthesis and structural characterization of products condensation 4-carboxy-1-(4-styrylcarbonylphenyl)-2-pyrrolidinones with hydrazines*. **2007**; Vol. 2007(15), 303-314.

36. Ansel, H. C.; Norred, W. P.; Roth, I. L., Antimicrobial Activity of Dimethyl Sulfoxide Against *Escherichia coli*, *Pseudomonas aeruginosa*, and *Bacillus megaterium*.



Journal of Pharmaceutical Sciences **1969**, 58 (7), 836-839.

37. Mohammad, H.; Younis, W.; Chen, L.; Peters, C. E.; Pogliano, J.; Pogliano, K.;

Cooper, B.; Zhang, J.; Mayhoub, A.; Oldfield, E.; Cushman, M.; Seleem, M. N.,

Phenylthiazole Antibacterial Agents Targeting Cell Wall Synthesis Exhibit Potent

Activity in Vitro and in Vivo against Vancomycin-Resistant Enterococci. *Journal of*

Medicinal Chemistry **2017**, 60 (6), 2425-2438.

38. Chang, S.-Y.; Ko, T.-P.; Chen, A. P.-C.; Wang, A. H.-J.; Liang, P.-H., Substrate

binding mode and reaction mechanism of undecaprenyl pyrophosphate synthase

deduced from crystallographic studies. *Protein Science* **2004**, 13 (4), 971-978.

39. Chang, S.-Y.; Ko, T.-P.; Liang, P.-H.; Wang, A. H.-J., Catalytic Mechanism

Revealed by the Crystal Structure of Undecaprenyl Pyrophosphate Synthase in

Complex with Sulfate, Magnesium, and Triton. *Journal of Biological Chemistry* **2003**,

278 (31), 29298-29307.

40. Workman, S. D.; Worrall, L. J.; Strynadka, N. C. J., Crystal structure of an

intramembranal phosphatase central to bacterial cell-wall peptidoglycan biosynthesis

and lipid recycling. *Nature Communications* **2018**, 9 (1), Article number : 1159.

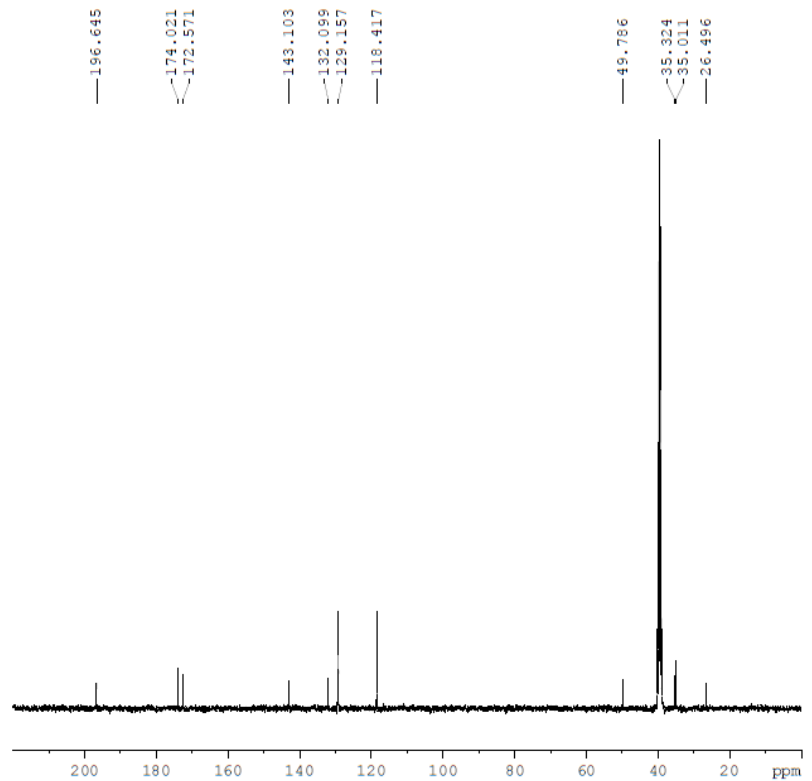
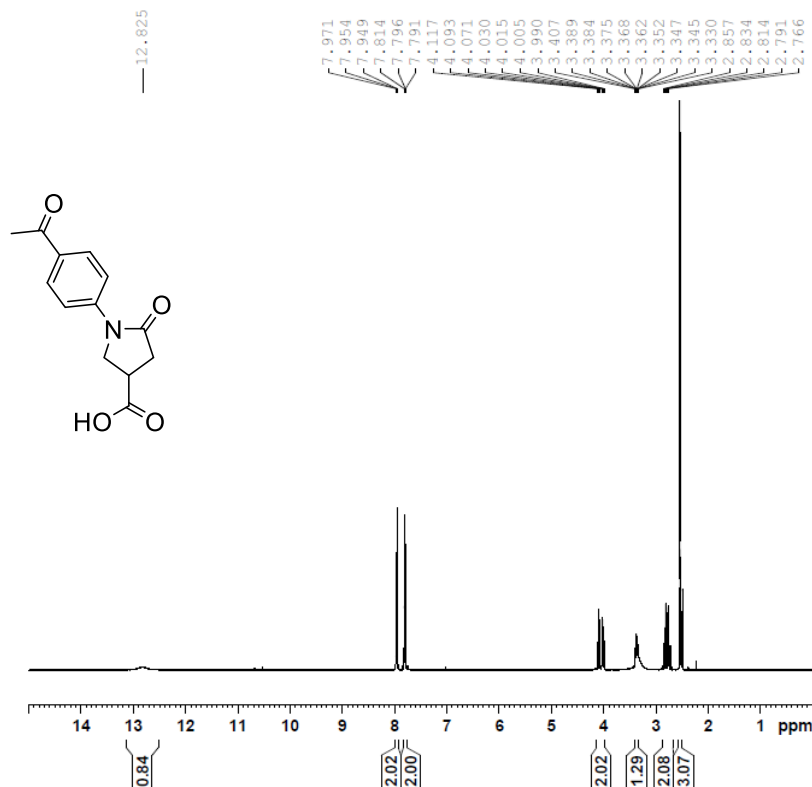
41. Cornish, K.; Siler, D. J.; Grosjean, O.-K. K., Immunoinhibition of rubber

particle-bound cis-prenyl transferases in ficus elastica and parthenium argentatum.

Phytochemistry **1994**, 35 (6), 1425-1428.

SPECTRUM

^1H (top) and ^{13}C (bottom) spectra of compound 1



Current Data Parameters
 NAME compound 1
 EXPNO 1
 PROCNO 1

F2 - Acquisition Parameters
 Date_ 20170808
 Time_ 15.37 h
 INSTRUM spect
 PROBHD Z108618_0411 (
 PULPROG zg30
 TD 32768
 SOLVENT DMSO
 NS 10
 DS 0
 SWH 8802.817 Hz
 FIDRES 0.537281 Hz
 AQ 1.8612224 sec
 RG 165.3
 DW 56.800 usec
 DE 14.47 usec
 TE 298.9 K
 D1 1.00000000 sec
 TD0 1
 SFO1 400.1328009 MHz
 NUC1 ^1H
 P1 15.50 usec
 PLW1 10.89999962 W

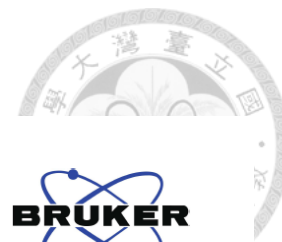
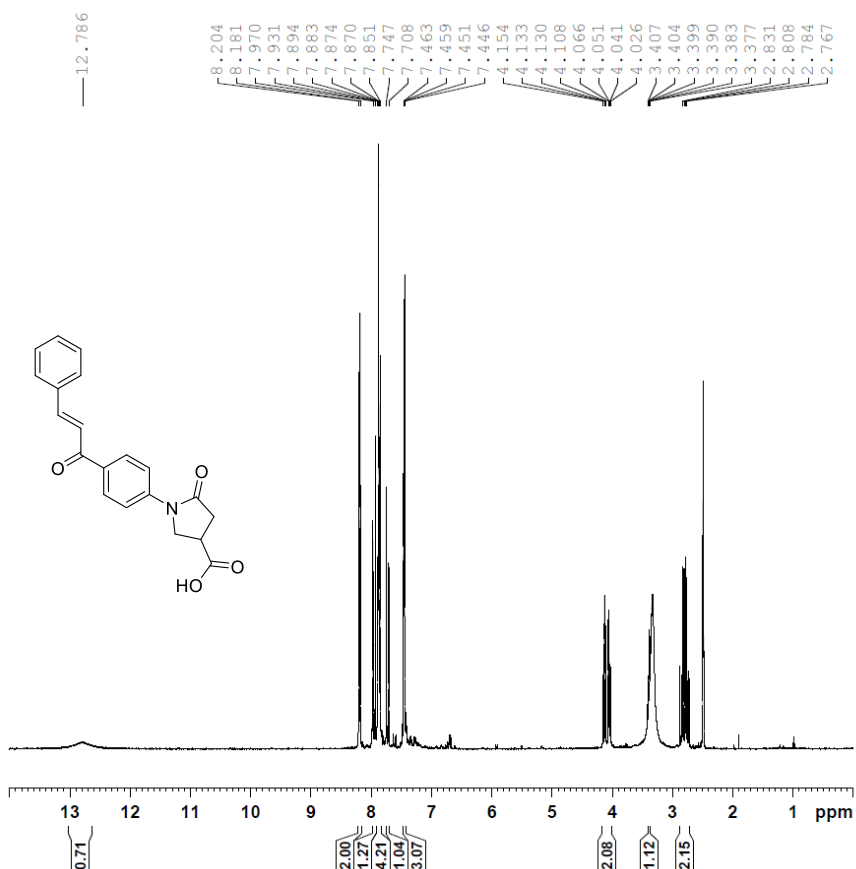
F2 - Processing parameters
 SI 131072
 SF 400.1300076 MHz
 WDW EM
 SSB 0
 LB 0 Hz
 GB 0
 PC 1.00

Current Data Parameters
 NAME compound 1
 EXPNO 2
 PROCNO 1

F2 - Acquisition Parameters
 Date_ 20170808
 Time_ 15.58 h
 INSTRUM spect
 PROBHD Z108618_0411 (
 PULPROG zgpg30
 TD 65536
 SOLVENT DMSO
 NS 123
 DS 4
 SWH 28409.092 Hz
 FIDRES 0.866977 Hz
 AQ 1.1534336 sec
 RG 212.49
 DW 17.600 usec
 DE 6.50 usec
 TE 298.9 K
 D1 2.00000000 sec
 D11 0.03000000 sec
 TD0 1
 SFO1 100.6258487 MHz
 NUC1 ^{13}C
 P1 10.50 usec
 PLW1 47.29999924 W
 SFO2 400.1316005 MHz
 NUC2 ^1H
 CPDPRG[2] waltz16
 PCPD2 90.00 usec
 PLW2 10.89999962 W
 PLW12 0.32330000 W
 PLW13 0.16236000 W

F2 - Processing parameters
 SI 32768
 SF 100.6128735 MHz
 WDW EM
 SSB 0
 LB 3.00 Hz
 GB 0
 PC 1.40

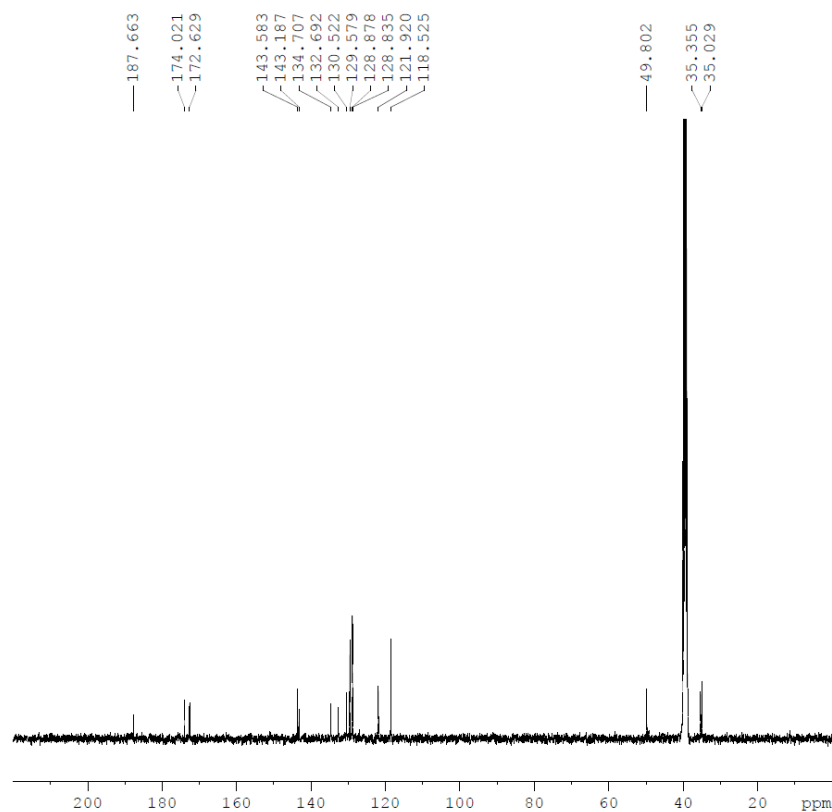
^1H (top) and ^{13}C (bottom) spectura of compound 2a



Current Data Parameters
 NAME compound 2a
 EXPNO 11111
 PROCNO 1

F2 - Acquisition Parameters
 Date_ 20180921
 Time 15.17 h
 INSTRUM spect
 PROBHD Z108618_0411 (
 PULPROG zg30
 TD 32768
 SOLVENT DMSO
 NS 20
 DS 0
 SWH 8802.817 Hz
 FIDRES 0.537281 Hz
 AQ 1.8612224 sec
 RG 31.38
 DW 56.800 usec
 DE 14.47 usec
 TE 300.4 K
 D1 1.00000000 sec
 TD0 1
 SFO1 400.1328009 MHz
 NUC1 1H
 P1 15.50 usec
 PLW1 10.89999962 W

F2 - Processing parameters
 SI 131072
 SF 400.1300074 MHz
 WDW EM
 SSB 0
 LB 0 Hz
 GB 0
 PC 1.00

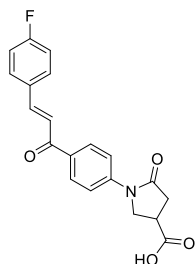
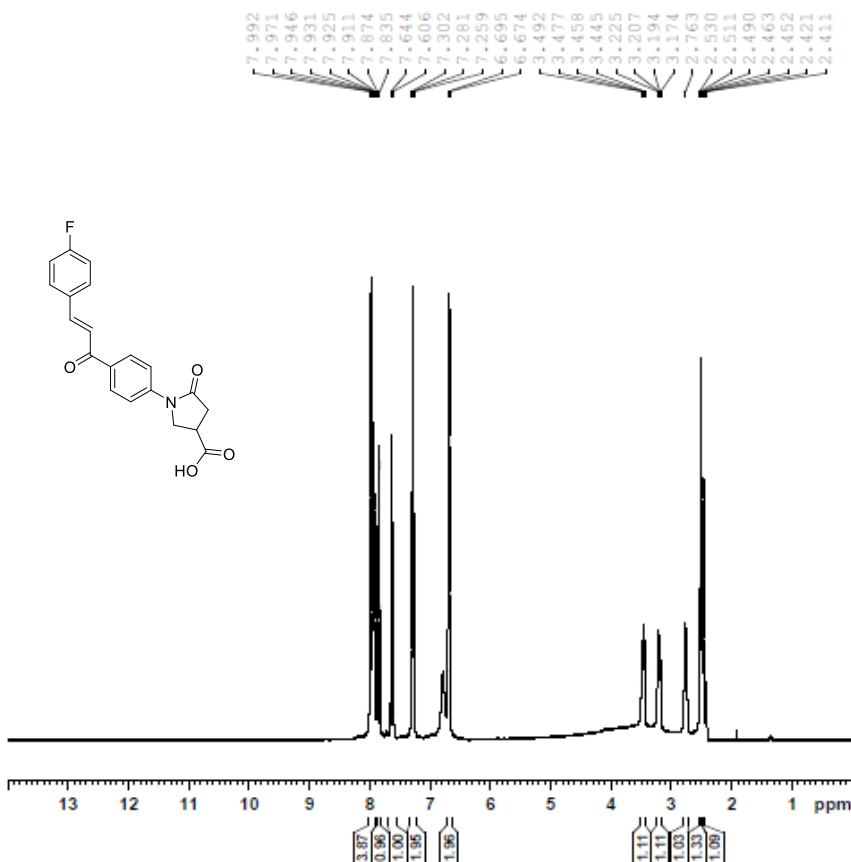


Current Data Parameters
 NAME compound 2a
 EXPNO 11112
 PROCNO 1

F2 - Acquisition Parameters
 Date_ 20190514
 Time 13.40 h
 INSTRUM spect
 PROBHD Z108618_0411 (
 PULPROG zgpg30
 TD 65336
 SOLVENT DMSO
 NS 604
 DS 4
 SWH 28409.092 Hz
 FIDRES 0.866977 Hz
 AQ 1.1534336 sec
 RG 212.49
 DW 17.600 usec
 DE 6.50 usec
 TE 297.5 K
 D1 2.00000000 sec
 D11 0.03000000 sec
 TD0 1
 SFO1 100.6258487 MHz
 NUC1 13C
 P1 10.50 usec
 PLW1 42.50000000 W
 SFO2 400.1316005 MHz
 NUC2 1H
 CPDPRG[2] waltz16
 PCPD2 90.00 usec
 PLW2 9.89999962 W
 PLW12 0.29363999 W
 PLW13 0.14747000 W

F2 - Processing parameters
 SI 32768
 SF 100.6128198 MHz
 WDW EM
 SSB 0
 LB 3.00 Hz
 GB 0
 PC 1.40

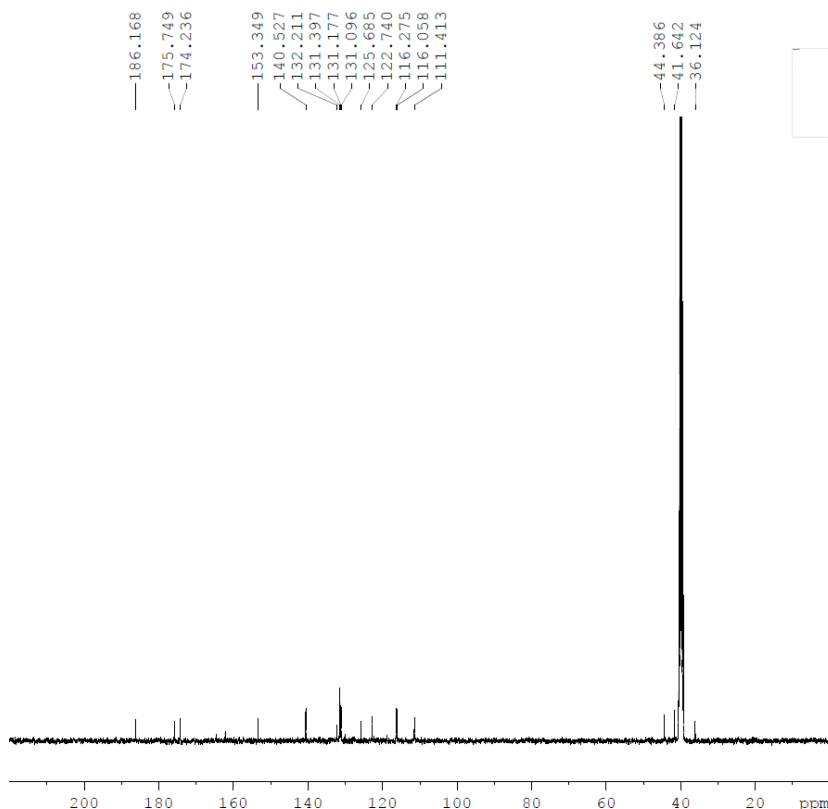
^1H (top) and ^{13}C (bottom) spectra of compound 2b



Current Data Parameters
NAME compound 2b
EXPNO 1
PROCNO 1

F2 - Acquisition Parameters
Date_ 20171220
Time 16.36 h
INSTRUM spect
PROBHD Z108618_0411 (
PULPROG zg30
TD 32768
SOLVENT DMSO
NS 20
DS 0
SWH 8802.817 Hz
FIDRES 0.537281 Hz
AQ 1.8612224 sec
RG 118.08
DW 56.800 usec
DE 14.47 usec
TE 298.9 K
D1 1.00000000 sec
TD0 1
SFO1 400.1328009 MHz
NUC1 1H
P1 15.50 usec
PLW1 10.89999962 W

F2 - Processing parameters
SI 131072
SF 400.1299979 MHz
WDW EM
SSB 0
LB 0 Hz
GB 0
PC 1.00

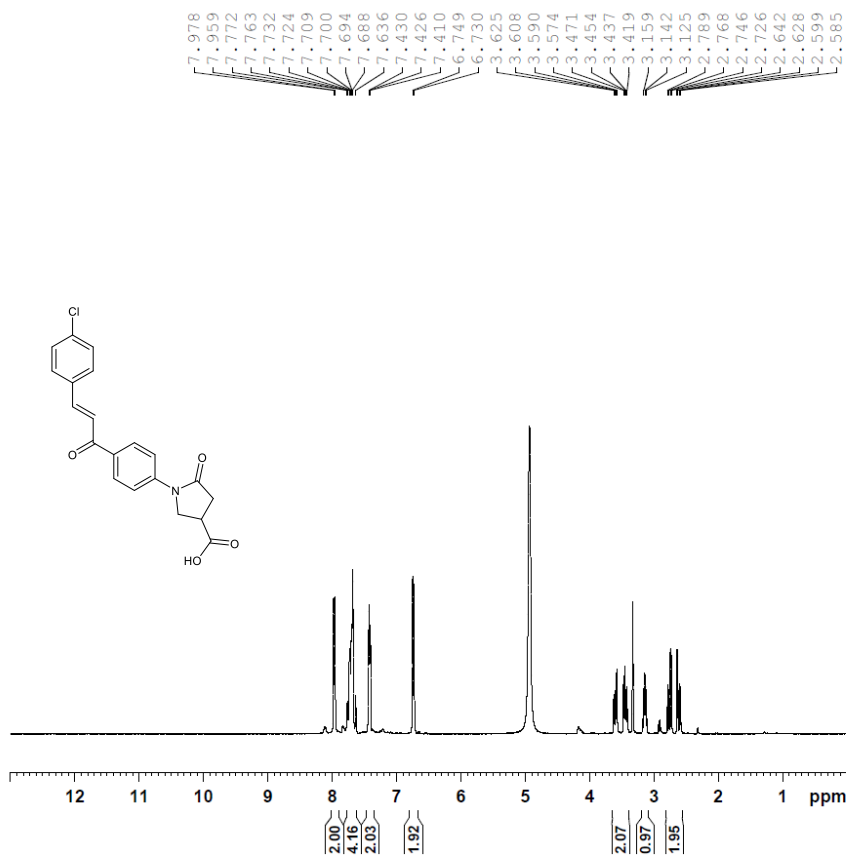


Current Data Parameters
NAME compound 2b
EXPNO 12
PROCNO 1

F2 - Acquisition Parameters
Date_ 20190505
Time 10.36 h
INSTRUM spect
PROBHD Z108618_0411 (
PULPROG zgpg30
TD 65536
SOLVENT DMSO
NS 500
DS 4
SWH 28409.092 Hz
FIDRES 0.866977 Hz
AQ 1.1534336 sec
RG 212.49
DW 17.600 usec
DE 6.50 usec
TE 297.8 K
D1 2.00000000 sec
D11 0.03000000 sec
TD0 1
SFO1 100.6258487 MHz
NUC1 13C
P1 10.50 usec
PLW1 42.50000000 W
SFO2 400.1316005 MHz
NUC2 1H
CPDPRG2 waltz16
PCPD2 90.00 usec
PLW2 9.89999962 W
PLW12 0.29363999 W
PLW13 0.14747000 W

F2 - Processing parameters
SI 32768
SF 100.6127792 MHz
WDW EM
SSB 0
LB 3.00 Hz
GB 0
PC 1.40

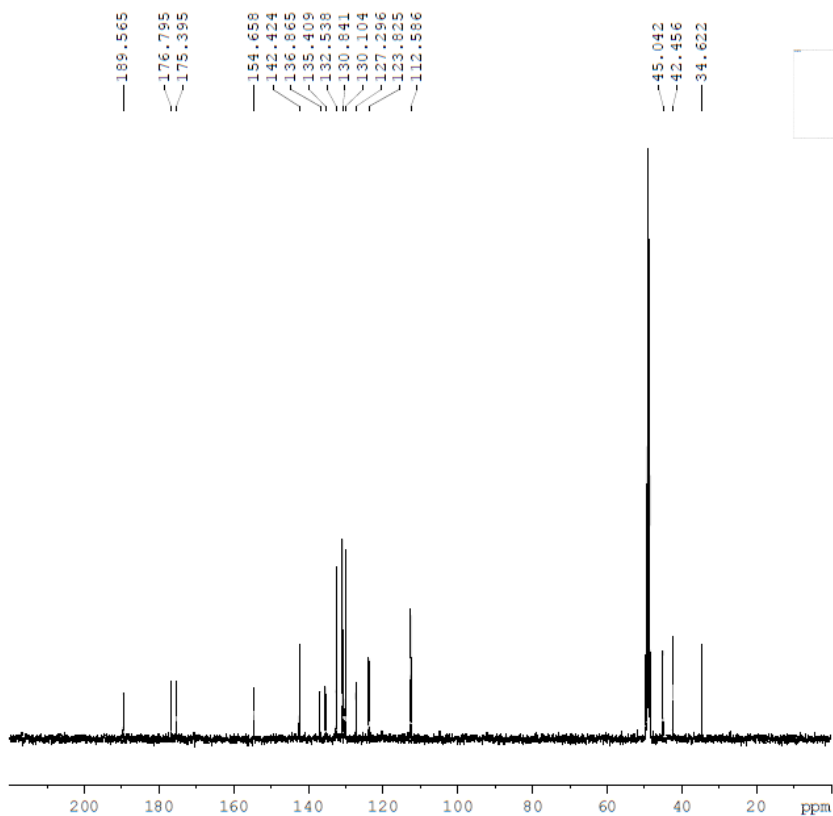
^1H (top) and ^{13}C (bottom) spectra of compound 2c



Current Data Parameters
 NAME compound 2c
 EXPNO 1
 PROCNO 1

F2 - Acquisition Parameters
 Date_ 20170830
 Time_ 12.59 h
 INSTRUM spect
 PROBHD Z108618_0411 (
 PULPROG zg30
 TD 32768
 SOLVENT MeOD
 NS 20
 DS 0
 SWH 8802.817 Hz
 FIDRES 0.537281 Hz
 AQ 1.8612224 sec
 RG 118.08
 DW 56.800 usec
 DE 14.47 usec
 TE 298.6 K
 D1 1.00000000 sec
 TD0 1
 SFO1 400.1328009 MHz
 NUC1 ^1H
 P1 15.50 usec
 PLW1 10.89999962 W

F2 - Processing parameters
 SI 131072
 SF 400.1300000 MHz
 WDW EM
 SSB 0
 LB 0 Hz
 GB 0
 PC 1.00

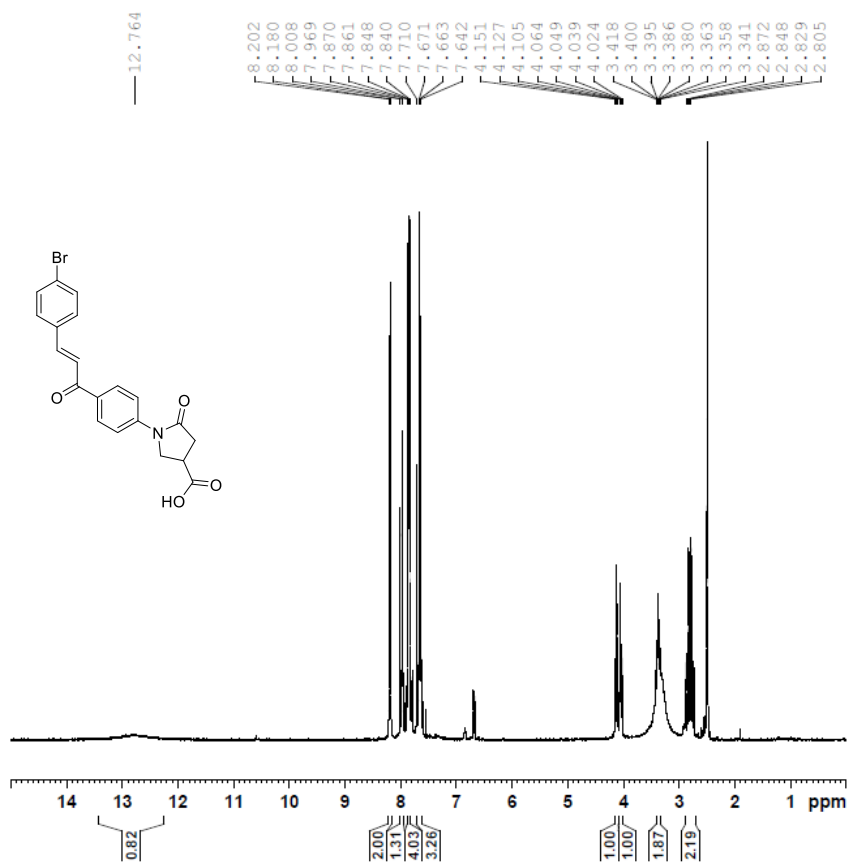


Current Data Parameters
 NAME compound 2c
 EXPNO 3
 PROCNO 1

F2 - Acquisition Parameters
 Date_ 20170830
 Time_ 13.24 h
 INSTRUM spect
 PROBHD Z108618_0411 (
 PULPROG zgpg30
 TD 65536
 SOLVENT MeOD
 NS 2
 DS 4
 SWH 28409.092 Hz
 FIDRES 0.866977 Hz
 AQ 1.1534336 sec
 RG 212.49
 DW 17.600 usec
 DE 6.50 usec
 TE 299.3 K
 D1 2.00000000 sec
 D11 0.03000000 sec
 TD0 1
 SFO1 100.6258487 MHz
 NUC1 ^{13}C
 P1 10.50 usec
 PLW1 47.29999924 W
 SFO2 400.1316005 MHz
 NUC2 ^1H
 CPDPRG[2] waltz16
 ECPD2 90.00 usec
 ELW2 10.89999962 W
 ELW12 0.32330000 W
 ELW13 0.16236000 W

F2 - Processing parameters
 SI 32768
 SF 100.6126328 MHz
 WDW EM
 SSB 0
 LB 3.00 Hz
 GB 0
 PC 1.40

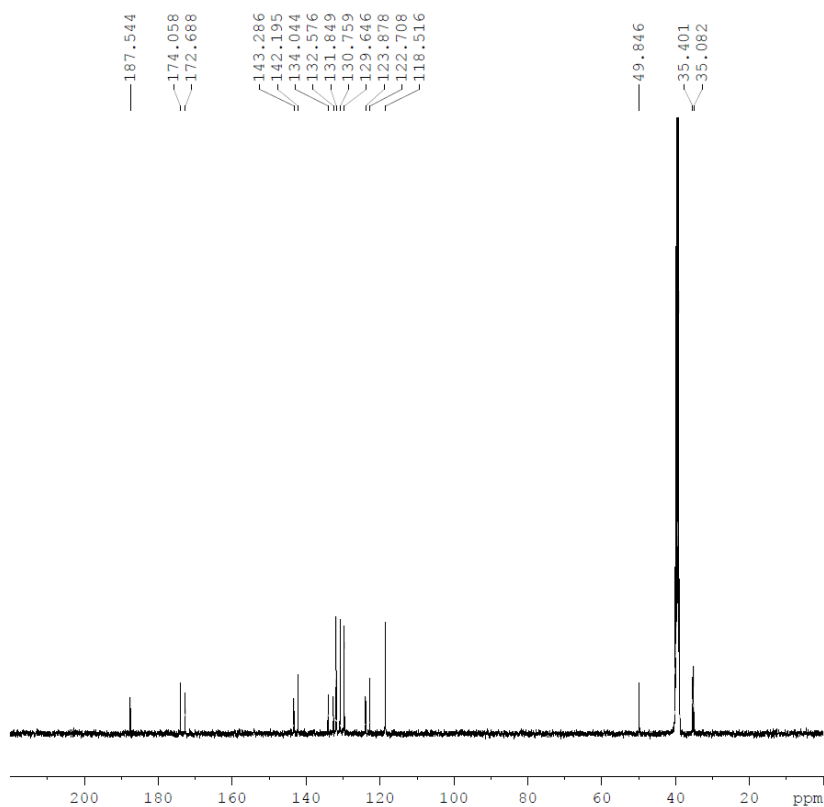
^1H (top) and ^{13}C (bottom) spectra of compound 2d



Current Data Parameters
 NAME compound 2d
 EXPNO 111
 PROCNO 1

F2 - Acquisition Parameters
 Date_ 20180123
 Time 16.47 h
 INSTRUM spect
 PROBHD Z108618_0411 (
 PULPROG zg30
 TD 32768
 SOLVENT DMSO
 NS 20
 DS 0
 SWH 8802.817 Hz
 FIDRES 0.537281 Hz
 AQ 1.8612224 sec
 RG 188.2
 DW 56.800 usec
 DE 14.47 usec
 TE 298.6 K
 D1 1.0000000 sec
 TD0 1
 SFO1 400.1328009 MHz
 NUC1 ^1H
 P1 15.50 usec
 PLW1 10.89999962 W

F2 - Processing parameters
 SI 131072
 SF 400.1300078 MHz
 WDW EM
 SSB 0
 LB 0 Hz
 GB 0
 PC 1.00

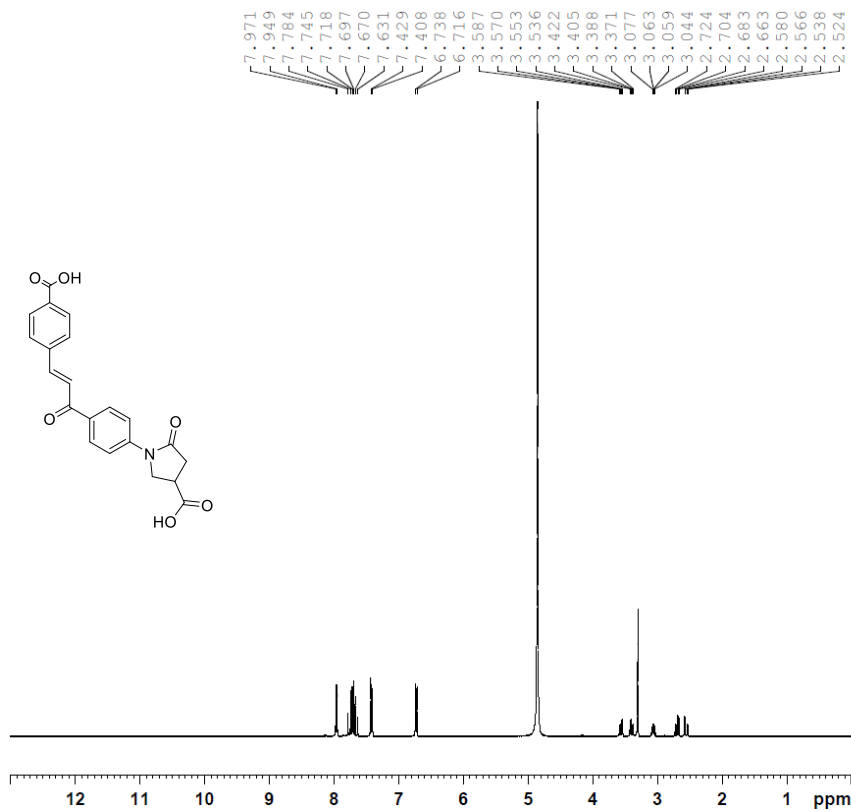
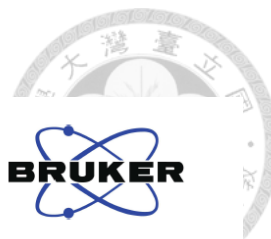


Current Data Parameters
 NAME compound 2d
 EXPNO 113
 PROCNO 1

F2 - Acquisition Parameters
 Date_ 20190508
 Time 16.34 h
 INSTRUM spect
 PROBHD Z108618_0411 (
 PULPROG zgpg30
 TD 65536
 SOLVENT DMSO
 NS 500
 DS 4
 SWH 28409.092 Hz
 FIDRES 0.866977 Hz
 AQ 1.1534336 sec
 RG 212.49
 DW 17.600 usec
 DE 6.50 usec
 TE 297.8 K
 D1 2.0000000 sec
 D11 0.03000000 sec
 TD0 1
 SFO1 100.6258487 MHz
 NUC1 ^{13}C
 P1 10.50 usec
 PLW1 42.50000000 W
 SFO2 400.1316005 MHz
 NUC2 ^1H
 CPDPRG[2] waltz16
 PCPD2 90.00 usec
 PLW2 9.89999962 W
 PLW12 0.29363999 W
 PLW13 0.14747000 W

F2 - Processing parameters
 SI 32768
 SF 100.6128179 MHz
 WDW EM
 SSB 0
 LB 3.00 Hz
 GB 0
 PC 1.40

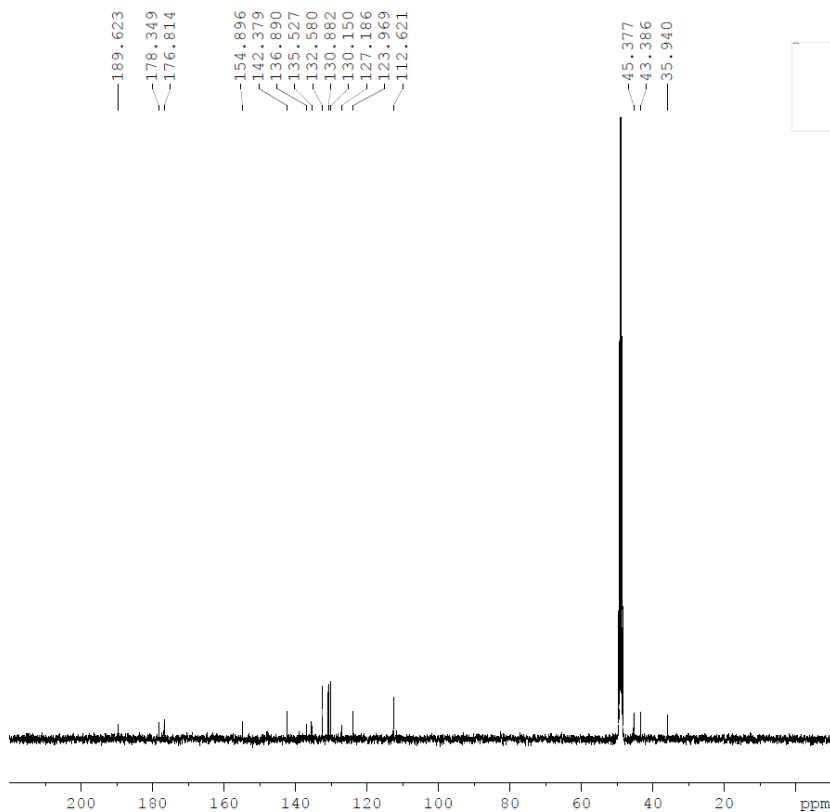
^1H (top) and ^{13}C (bottom) spectra of compound 2e



Current Data Parameters
 NAME compound 2e
 EXPNO 11
 PROCNO 1

F2 - Acquisition Parameters
 Date_ 20170922
 Time 16.04 h
 INSTRUM spect
 PROBHD Z108618_0411 (
 PULPROG zg30
 TD 32768
 SOLVENT MeOD
 NS 20
 DS 0
 SWH 8802.817 Hz
 FIDRES 0.537281 Hz
 AQ 1.8612224 sec
 RG 188.2
 DW 56.800 usec
 DE 14.47 usec
 TE 299.0 K
 D1 1.00000000 sec
 TD0 1
 SFO1 400.1328009 MHz
 NUC1 ^1H
 P1 15.50 usec
 PLW1 10.89999962 W

F2 - Processing parameters
 SI 131072
 SF 400.1300121 MHz
 WDW EM
 SSB 0
 LB 0 Hz
 GB 0
 PC 1.00

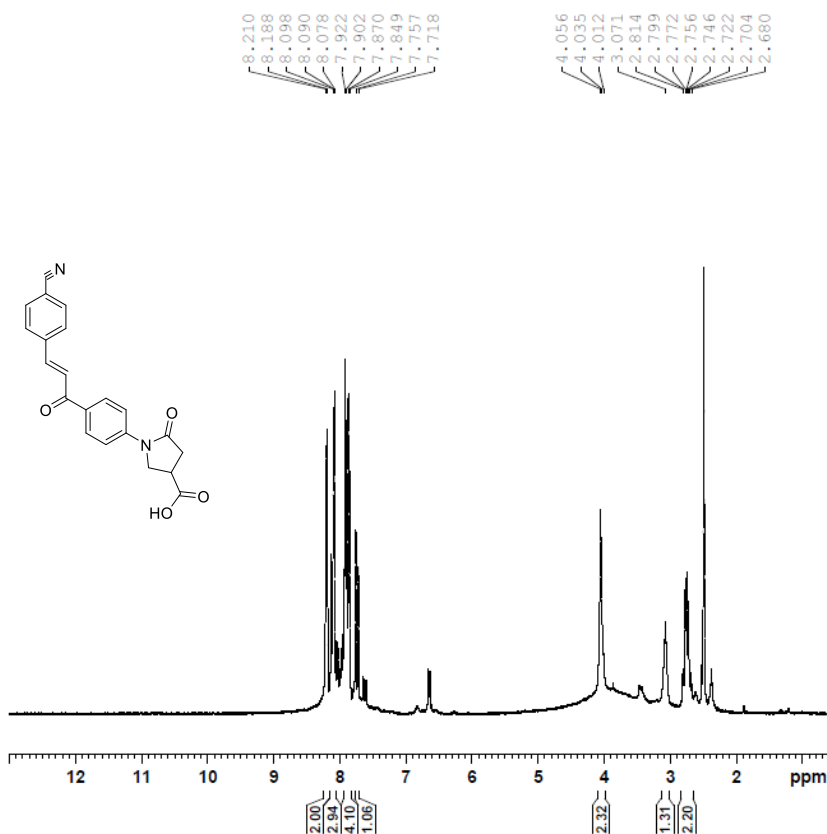


Current Data Parameters
 NAME compound 2e
 EXPNO 22
 PROCNO 1

F2 - Acquisition Parameters
 Date_ 20170922
 Time 17.01 h
 INSTRUM spect
 PROBHD Z108618_0411 (
 PULPROG zgpg30
 TD 65536
 SOLVENT MeOD
 NS 443
 DS 4
 SWH 28409.092 Hz
 FIDRES 0.866977 Hz
 AQ 1.1534336 sec
 RG 212.49
 DW 17.600 usec
 DE 6.50 usec
 TE 299.3 K
 D1 2.00000000 sec
 D11 0.03000000 sec
 TD0 1
 SFO1 100.6258487 MHz
 NUC1 ^{13}C
 P1 10.50 usec
 PLW1 47.29999924 W
 SFO2 400.1316005 MHz
 NUC2 ^1H
 CPDPRG[2] waltz16
 PCPD2 90.00 usec
 PLW2 10.89999962 W
 PLW12 0.32330000 W
 PLW13 0.16236000 W

F2 - Processing parameters
 SI 32768
 SF 100.6126279 MHz
 WDW EM
 SSB 0
 LB 3.00 Hz
 GB 0
 PC 1.40

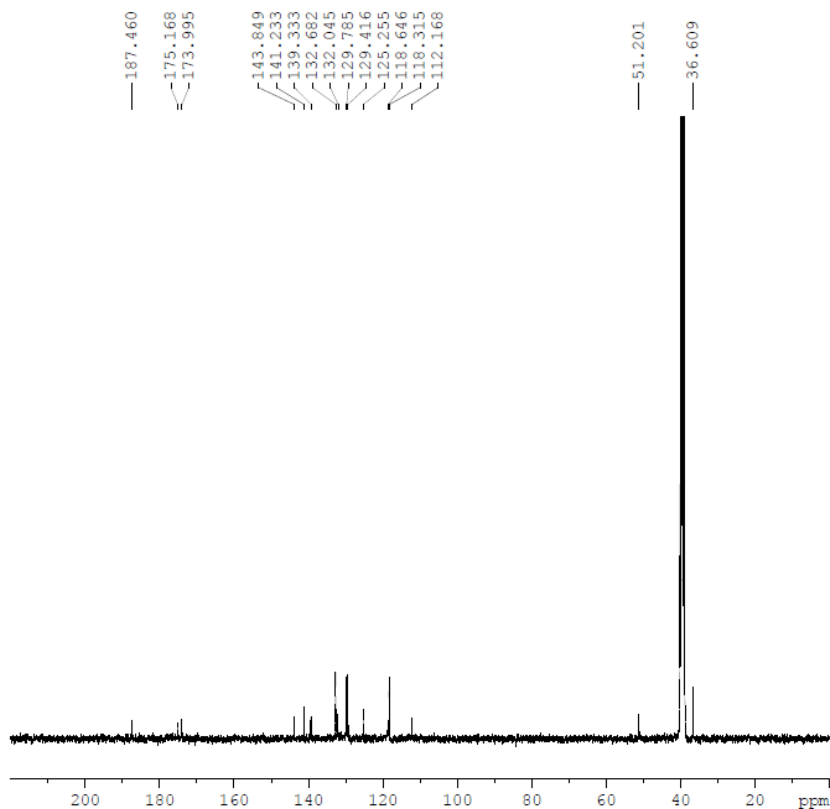
^1H (top) and ^{13}C (bottom) spectra of compound 2f



Current Data Parameters
 NAME compound 2f
 EXPNO 1111
 PROCNO 1

F2 - Acquisition Parameters
 Date_ 20190501
 Time 16.22 h
 INSTRUM spect
 PROBHD Z108618_0411 (
 PULPROG zg30
 TD 32768
 SOLVENT DMSO
 NS 20
 DS 0
 SWH 8802.817 Hz
 FIDRES 0.537281 Hz
 AQ 1.8612224 sec
 RG 165.3
 DW 56.800 usec
 DE 14.47 usec
 TE 297.1 K
 D1 1.00000000 sec
 TD0 1
 SFO1 400.1328009 MHz
 NUC1 ^1H
 P1 15.50 usec
 PLW1 9.89999962 W

F2 - Processing parameters
 SI 131072
 SF 400.1300077 MHz
 WDW EM
 SSB 0
 LB 0 Hz
 GB 0
 PC 1.00

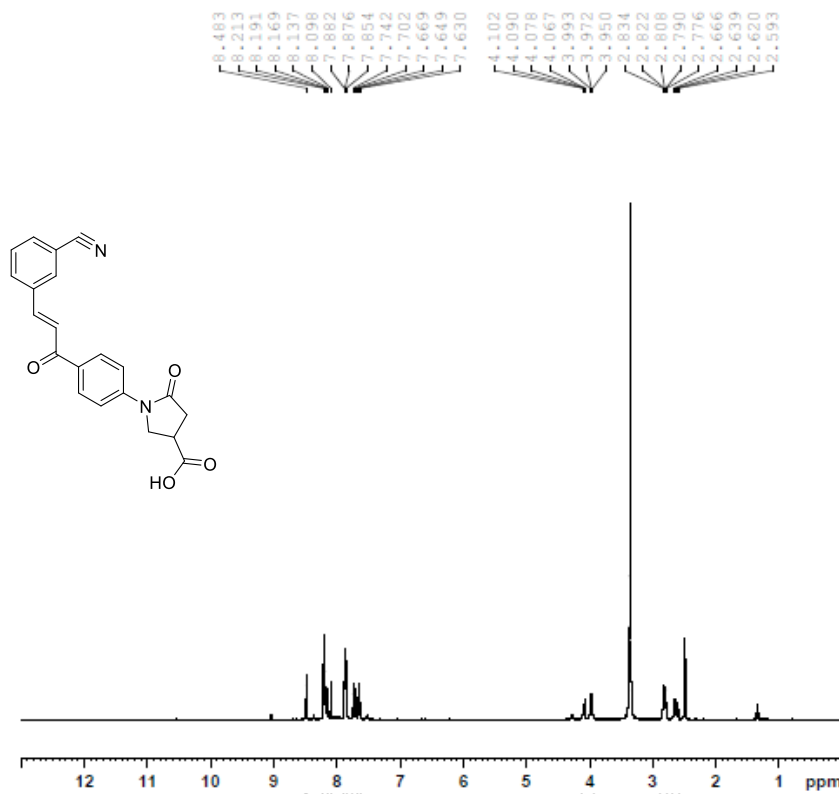


Current Data Parameters
 NAME compound 2f
 EXPNO 11112
 PROCNO 1

F2 - Acquisition Parameters
 Date_ 20190507
 Time 17.47 h
 INSTRUM spect
 PROBHD Z108618_0411 (
 PULPROG zgpg30
 TD 65536
 SOLVENT DMSO
 NS 700
 DS 4
 SWH 28409.092 Hz
 FIDRES 0.866977 Hz
 AQ 1.1534336 sec
 RG 212.49
 DW 17.600 usec
 DE 6.50 usec
 TE 297.6 K
 D1 2.00000000 sec
 D11 0.03000000 sec
 TD0 1
 SFO1 100.6258487 MHz
 NUC1 ^{13}C
 P1 10.50 usec
 PLW1 42.50000000 W
 SFO2 400.1316005 MHz
 NUC2 ^1H
 CPDPRG2 waltz16
 PCPD2 90.00 usec
 PLW2 9.89999962 W
 PLW12 0.29363999 W
 PLW13 0.14747000 W

F2 - Processing parameters
 SI 32768
 SF 100.6128187 MHz
 WDW EM
 SSB 0
 LB 3.00 Hz
 GB 0
 PC 1.40

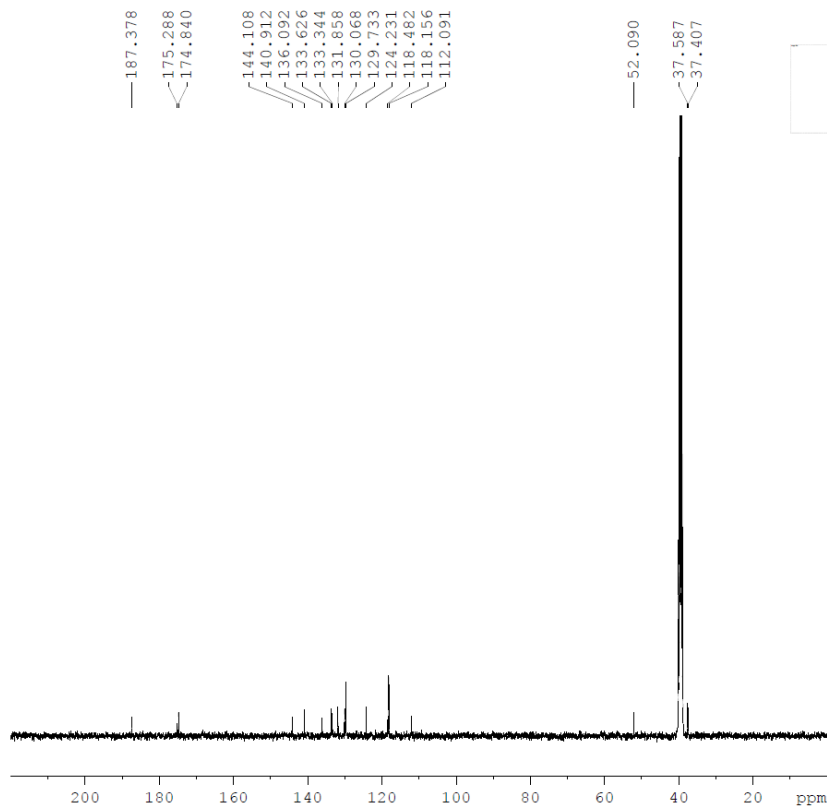
^1H (top) and ^{13}C (bottom) spectra of compound 2g



Current Data Parameters
 NAME compound 2g
 EXPNO 1111
 PROCNO 1

F2 - Acquisition Parameters
 Date_ 20190505
 Time 10.41 h
 INSTRUM spect
 PROBHD Z108618_0411 (
 PULPROG zg30
 TD 32768
 SOLVENT DMSO
 NS 20
 DS 0
 SWH 8802.817 Hz
 FIDRES 0.537281 Hz
 AQ 1.8612224 sec
 RG 165.3
 DW 56.800 usec
 DE 14.47 usec
 TE 297.6 K
 D1 1.0000000 sec
 TD0 1
 SFO1 400.1328009 MHz
 NUC1 ^1H
 P1 15.50 usec
 PLW1 9.89999962 W

F2 - Processing parameters
 SI 131072
 SF 400.1300080 MHz
 WDW EM
 SSB 0
 LB 0 Hz
 GB 0
 PC 1.00

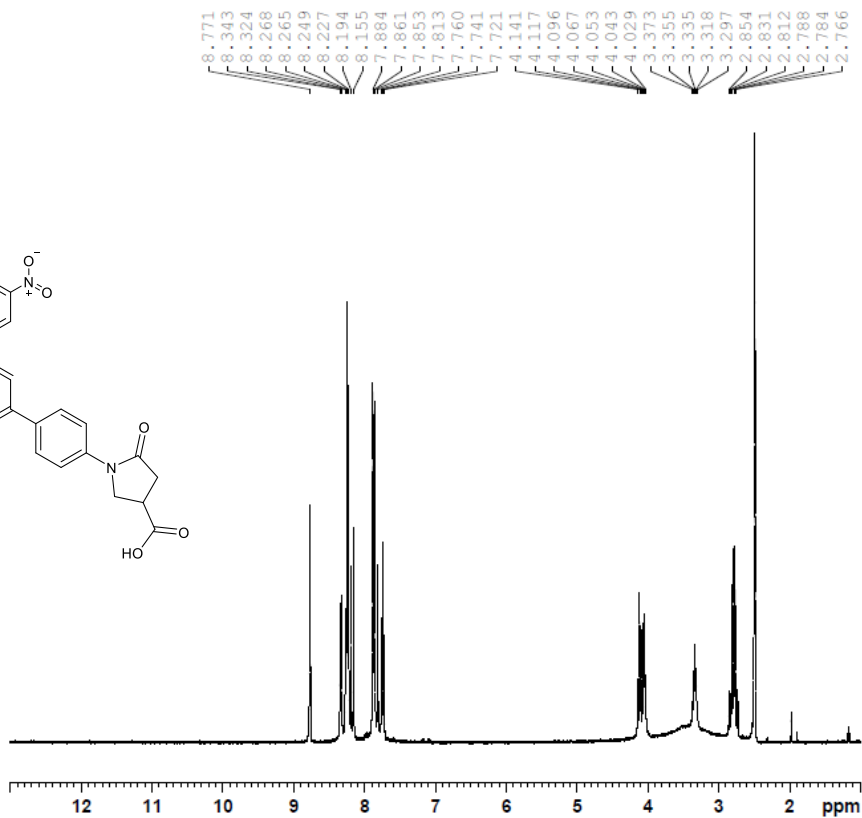
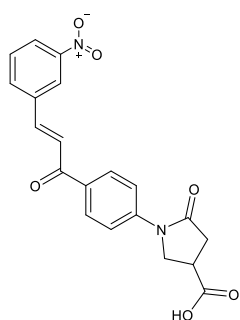


Current Data Parameters
 NAME compound 2g
 EXPNO 1112
 PROCNO 1

F2 - Acquisition Parameters
 Date_ 20190505
 Time 11.18 h
 INSTRUM spect
 PROBHD Z108618_0411 (
 PULPROG zgpg30
 TD 65536
 SOLVENT DMSO
 NS 600
 DS 4
 SWH 28409.092 Hz
 FIDRES 0.866977 Hz
 AQ 1.1534336 sec
 RG 212.49
 DW 17.600 usec
 DE 6.50 usec
 TE 298.0 K
 D1 2.0000000 sec
 D11 0.0300000 sec
 TD0 1
 SFO1 100.6258487 MHz
 NUC1 ^{13}C
 P1 10.50 usec
 PLW1 42.5000000 W
 SFO2 400.1316005 MHz
 NUC2 ^1H
 CPDPRG[2] waltz16
 ECPD2 90.00 usec
 PLW2 9.89999962 W
 PLW12 0.29363999 W
 PLW13 0.14747000 W

F2 - Processing parameters
 SI 32768
 SF 100.6128186 MHz
 WDW EM
 SSB 0
 LB 3.00 Hz
 GB 0
 PC 1.40

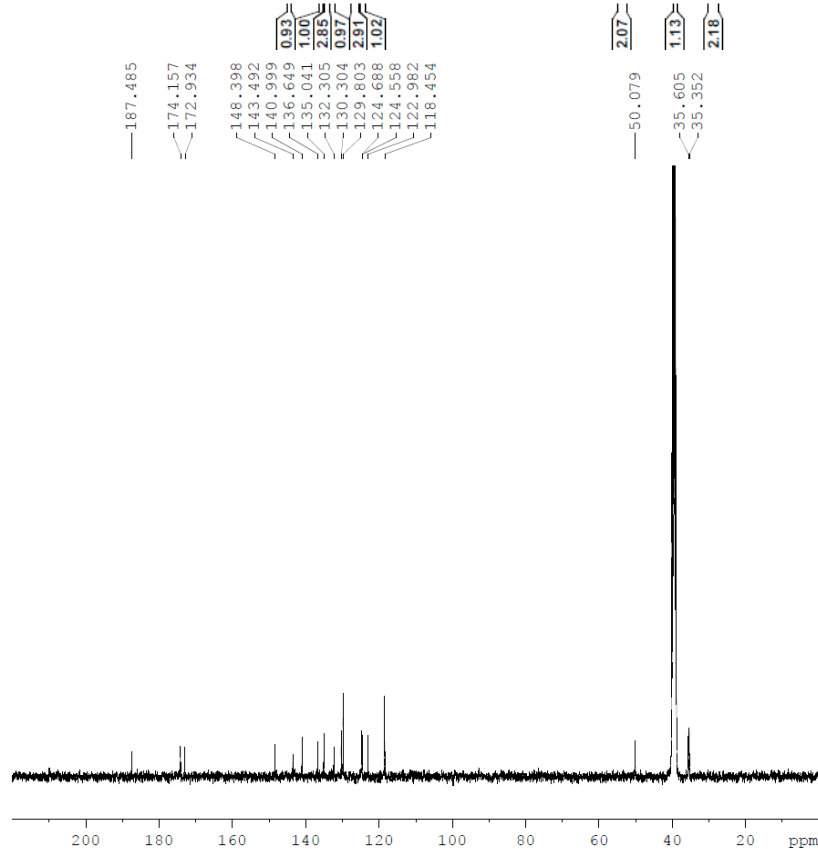
^1H (top) and ^{13}C (bottom) spectra of compound 2h



Current Data Parameters
 NAME compound 2h
 EXPNO 1
 PROCNO 1

F2 - Acquisition Parameters
 Date_ 20180130
 Time 16.32 h
 INSTRUM spect
 PROBHD Z108618_0411 (
 PULPROG zg30
 TD 32768
 SOLVENT DMSO
 NS 20
 DS 0
 SWH 8802.817 Hz
 FIDRES 0.537281 Hz
 AQ 1.8612224 sec
 RG 212.49
 DW 56.800 usec
 DE 14.47 usec
 TE 298.0 K
 D1 1.0000000 sec
 TD0 1
 SFO1 400.1328009 MHz
 NUC1 ^1H
 P1 15.50 usec
 PLW1 10.89999962 W

F2 - Processing parameters
 SI 131072
 SF 400.1300078 MHz
 WDW EM
 SSB 0
 LB 0 Hz
 GB 0
 PC 1.00

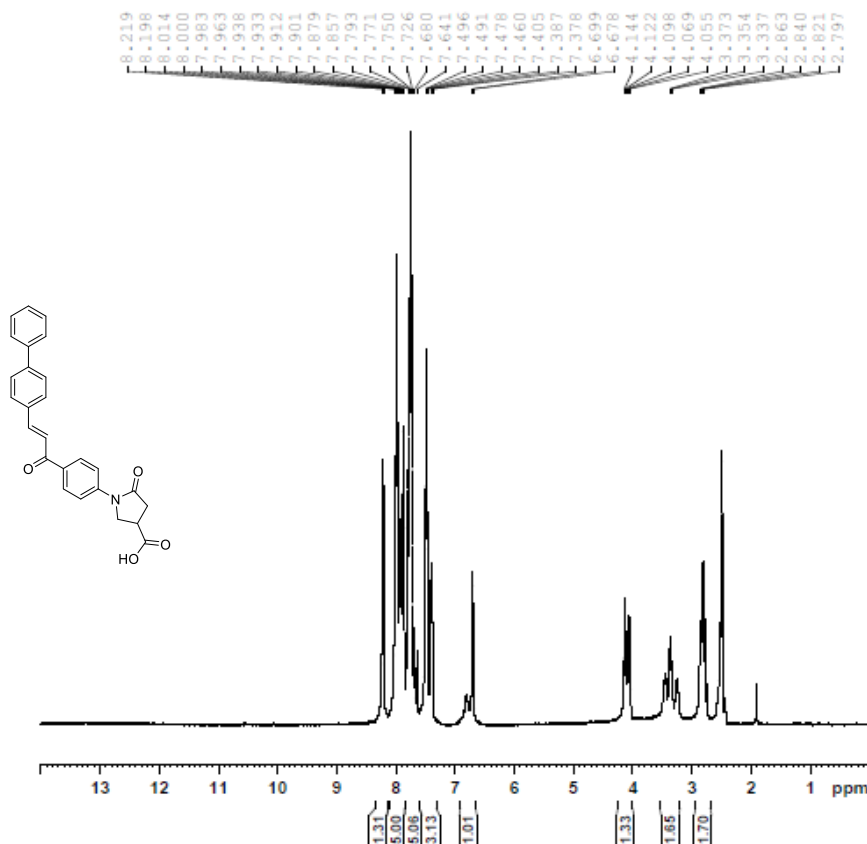


Current Data Parameters
 NAME compound 2h
 EXPNO 3
 PROCNO 1

F2 - Acquisition Parameters
 Date_ 20190509
 Time 14.51 h
 INSTRUM spect
 PROBHD Z108618_0411 (
 PULPROG zgpg30
 TD 65536
 SOLVENT DMSO
 NS 750
 DS 4
 SWH 28409.092 Hz
 FIDRES 0.866977 Hz
 AQ 1.1534336 sec
 RG 212.49
 DW 17.600 usec
 DE 6.50 usec
 TE 297.7 K
 D1 2.0000000 sec
 D11 0.0300000 sec
 TD0 1
 SFO1 100.6258487 MHz
 NUC1 ^{13}C
 P1 10.50 usec
 PLW1 42.5000000 W
 SFO2 400.1316005 MHz
 NUC2 ^1H
 CPDPRG2 waltz16
 PCPD2 90.00 usec
 PLW2 9.89999962 W
 PLW12 0.29363999 W
 PLW13 0.14747000 W

F2 - Processing parameters
 SI 32768
 SF 100.6128202 MHz
 WDW EM
 SSB 0
 LB 3.00 Hz
 GB 0
 PC 1.40

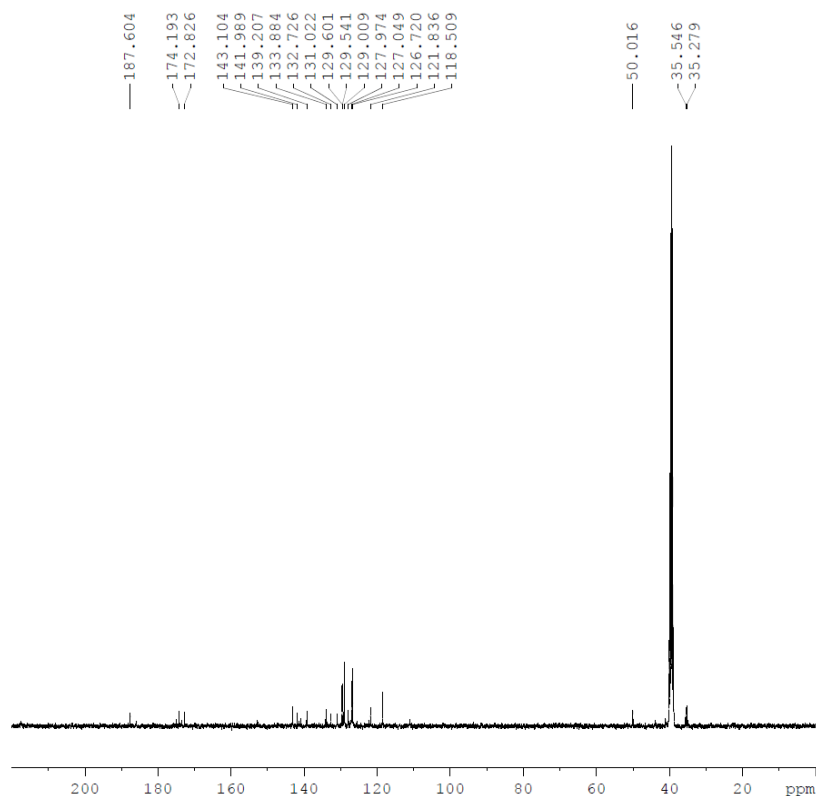
^1H (top) and ^{13}C (bottom) spectra of compound 2i



Current Data Parameters
 NAME compound 2i
 EXPNO 1
 PROCNO 1

F2 - Acquisition Parameters
 Date_ 20180313
 Time_ 15.12 h
 INSTRUM spect
 PROBHD Z108618_0411 (
 PULPROG zg30
 TD 32768
 SOLVENT DMSO
 NS 20
 DS 0
 SWH 8802.817 Hz
 FIDRES 0.537281 Hz
 AQ 1.8612224 sec
 RG 118.08
 DW 56.800 usec
 DE 14.47 usec
 TE 298.9 K
 D1 1.00000000 sec
 TD0 1
 SFO1 400.1328009 MHz
 NUC1 ^1H
 P1 15.50 usec
 PLW1 10.89999962 W

F2 - Processing parameters
 SI 131072
 SF 400.1300087 MHz
 WDW EM
 SSB 0
 LB 0 Hz
 GB 0
 PC 1.00

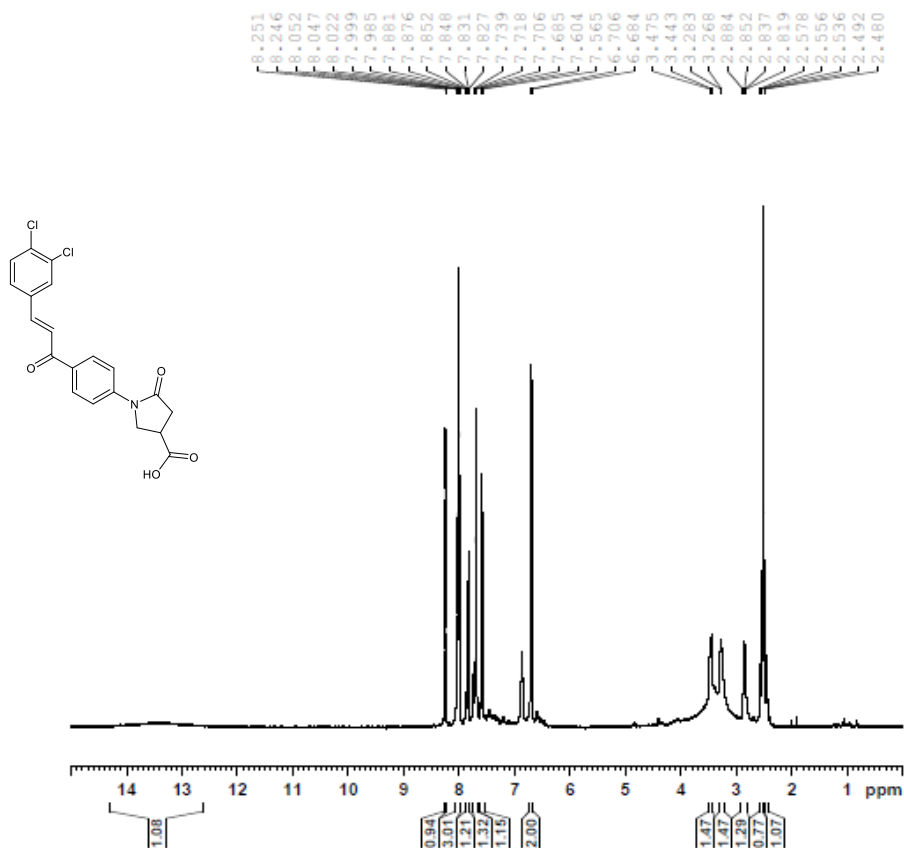


Current Data Parameters
 NAME compound 2i
 EXPNO 22
 PROCNO 1

F2 - Acquisition Parameters
 Date_ 20190510
 Time_ 14.27 h
 INSTRUM spect
 PROBHD Z108618_0411 (
 PULPROG zgpg30
 TD 65536
 SOLVENT DMSO
 NS 205
 DS 4
 SWH 28409.092 Hz
 FIDRES 0.866977 Hz
 AQ 1.1534336 sec
 RG 212.49
 DW 17.600 usec
 DE 6.50 usec
 TE 297.5 K
 D1 2.00000000 sec
 D11 0.03000000 sec
 TD0 1
 SFO1 100.6258487 MHz
 NUC1 ^{13}C
 F1 10.50 usec
 PLW1 42.50000000 W
 SFO2 400.1316005 MHz
 NUC2 ^1H
 CPDPRG[2] waltz16
 PCPD2 90.00 usec
 PLW2 9.89999962 W
 PLW12 0.29363999 W
 PLW13 0.14747000 W

F2 - Processing parameters
 SI 32768
 SF 100.6128183 MHz
 WDW EM
 SSB 0
 LB 3.00 Hz
 GB 0
 PC 1.40

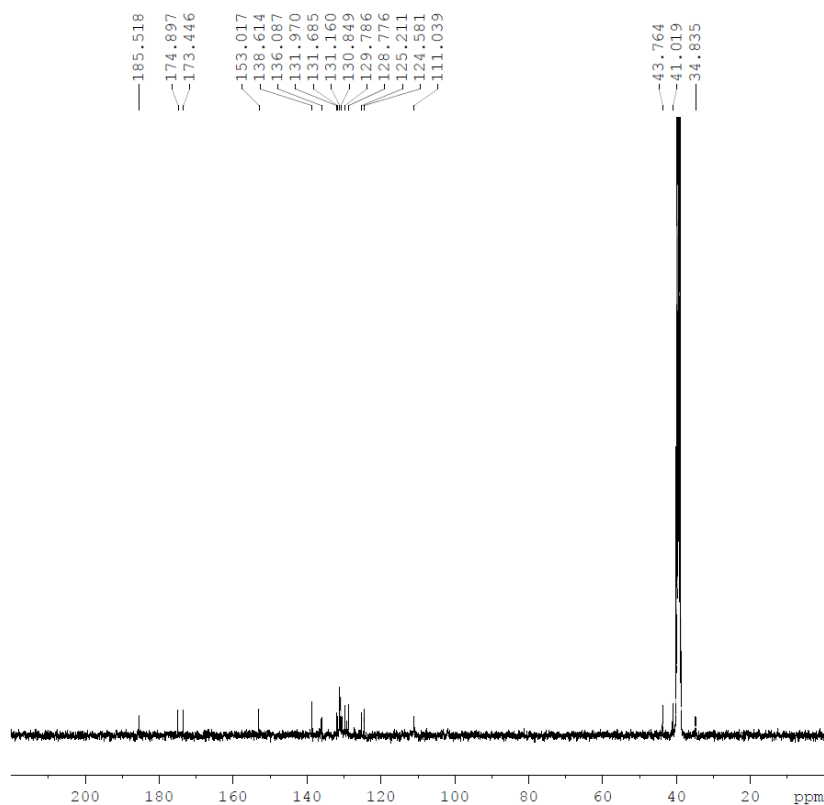
^1H (top) and ^{13}C (bottom) spectura of compound 2j



Current Data Parameters
 NAME compound 2j
 EXPNO 111
 PROCNO 1

F2 - Acquisition Parameters
 Date_ 20190222
 Time 13.53 h
 INSTRUM spect
 PROBHD Z108618_0411 (
 PULPROG zg30
 TD 32768
 SOLVENT DMSO
 NS 32
 DS 0
 SWH 8802.817 Hz
 FIDRES 0.537281 Hz
 AQ 1.8612224 sec
 RG 165.3
 DW 56.800 usec
 DE 14.47 usec
 TE 300.9 K
 D1 1.00000000 sec
 TD0 1
 SFO1 400.1328009 MHz
 NUC1 ^1H
 P1 15.50 usec
 PLW1 9.89999962 W

F2 - Processing parameters
 SI 131072
 SF 400.1300000 MHz
 WDW EM
 SSB 0
 LB 0 Hz
 GB 0
 PC 1.00

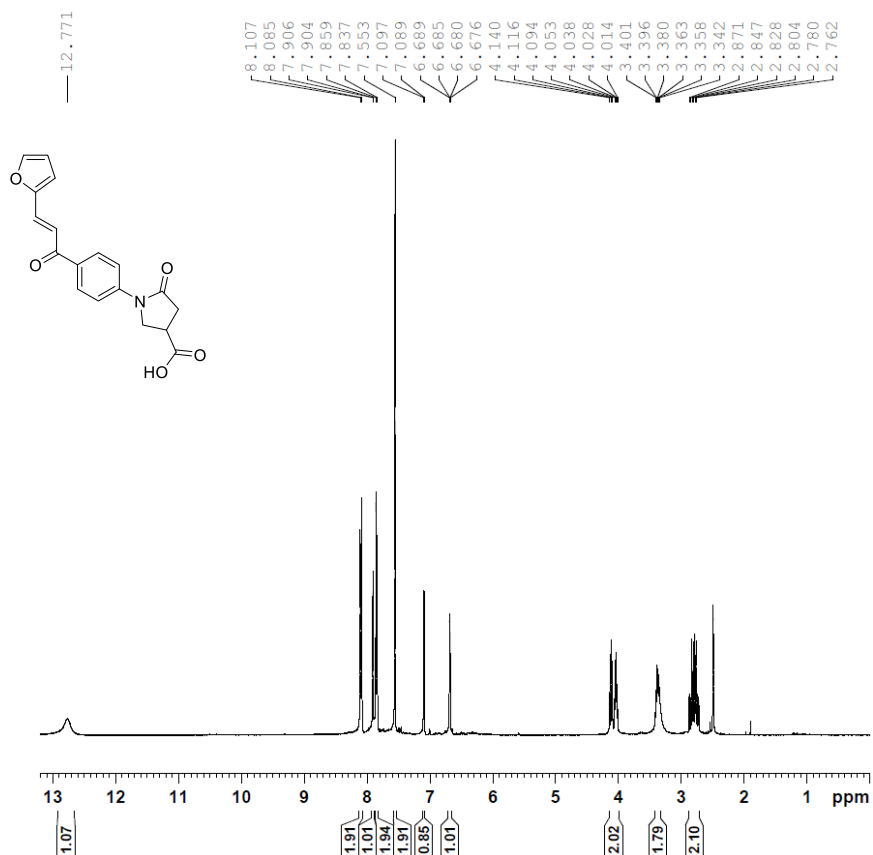
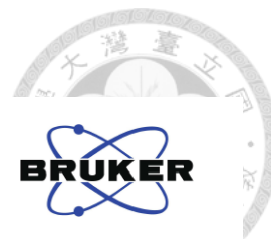


Current Data Parameters
 NAME compound 2j
 EXPNO 11112
 PROCNO 1

F2 - Acquisition Parameters
 Date_ 20190506
 Time 11.51 h
 INSTRUM spect
 PROBHD Z108618_0411 (
 PULPROG zgpg30
 TD 65536
 SOLVENT DMSO
 NS 600
 DS 4
 SWH 28409.092 Hz
 FIDRES 0.866977 Hz
 AQ 1.1534336 sec
 RG 212.49
 DW 17.600 usec
 DE 6.50 usec
 TE 297.7 K
 D1 2.00000000 sec
 D11 0.03000000 sec
 TD0 1
 SFO1 100.6258487 MHz
 NUC1 ^{13}C
 P1 10.50 usec
 PLW1 42.50000000 W
 SFO2 400.1316005 MHz
 NUC2 ^1H
 CPDPRG[2] waltz16
 PCPD2 90.00 usec
 PLW2 9.89999962 W
 PLW12 0.29363999 W
 PLW13 0.14747000 W

F2 - Processing parameters
 SI 32768
 SF 100.6128214 MHz
 WDW EM
 SSB 0
 LB 3.00 Hz
 GB 0
 PC 1.40

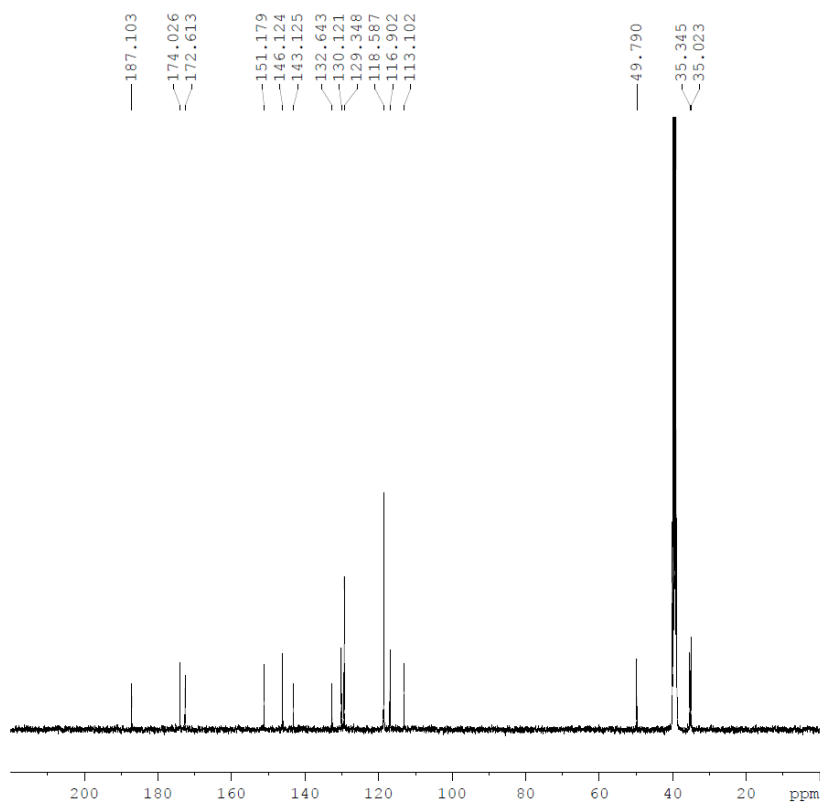
^1H (top) and ^{13}C (bottom) spectra of compound 2k



Current Data Parameters
 NAME compound 2k
 EXPNO 11111
 PROCNO 1

F2 - Acquisition Parameters
 Date_ 20190611
 Time 16.09 h
 INSTRUM spect
 PROBHD Z108618_0411 (
 PULPROG zg30
 TD 32768
 SOLVENT DMSO
 NS 20
 DS 0
 SWH 8802.817 Hz
 FIDRES 0.537281 Hz
 AQ 1.8612224 sec
 RG 133.5
 DW 56.800 usec
 DE 14.47 usec
 TE 297.0 K
 D1 1.00000000 sec
 TD0 1
 SFO1 400.1328009 MHz
 NUC1 ^1H
 P1 15.50 usec
 PLW1 9.89999962 W

F2 - Processing parameters
 SI 131072
 SF 400.1300074 MHz
 WDW EM
 SSB 0
 LB 0 Hz
 GB 0
 PC 1.00



Current Data Parameters
 NAME compound 2k
 EXPNO 11112
 PROCNO 1

F2 - Acquisition Parameters
 Date_ 20190611
 Time 16.51 h
 INSTRUM spect
 PROBHD Z108618_0411 (
 PULPROG zgpg30
 TD 65536
 SOLVENT DMSO
 NS 718
 DS 4
 SWH 28409.092 Hz
 FIDRES 0.866977 Hz
 AQ 1.1534336 sec
 RG 212.49
 DW 17.600 usec
 DE 6.50 usec
 TE 297.7 K
 D1 2.00000000 sec
 D11 0.03000000 sec
 TD0 1
 SFO1 100.6258487 MHz
 NUC1 ^{13}C
 P1 10.50 usec
 PLW1 42.50000000 W
 SFO2 400.1316005 MHz
 NUC2 ^1H
 CPDPRG[2] waltz16
 PCPD2 90.00 usec
 PLW2 9.89999962 W
 PLW12 0.29363999 W
 PLW13 0.14747000 W

F2 - Processing parameters
 SI 32768
 SF 100.6128180 MHz
 WDW EM
 SSB 0
 LB 3.00 Hz
 GB 0
 PC 1.40